Dear Editor,

we thank both reviewers for their useful comments. By following their suggestions, we will certainly be able to improve the quality of our manuscript. Below we attach a reply to all the points raised, where the reviewers' comments are in black, whereas our replies are indented in blue.

> To easily refer to the different reviews, we added a reference to each major point raised by the two Reviewers, labelled as "Rx.n", where "x" = n. of Reviewer, and "n" = n. of point.

EDITOR COMMENTS

The topic of your manuscript has been evaluated as of significant scientific interest and the overall presentation of good quality. However, both reviewers have raised some issues that I would urge you to constructively attend to, in particular, regarding the interpretation of DCM patterns produced by model simulations and how other processes (i.e. nutrient dynamics, grazing...) not discussed in the text affect patterns observed.

> We expanded the manuscripts as suggested by the Editor and Reviewers focusing on a better interpretation of the impact of nutrients and their interplay with different bio-optical models.
>
> This enabled a more complete and clearer overview of the patterns produced by the model compared to chlorophyll and radiometric data measured by BGC-Argo floats.
>
> We revised the introduction in order to make it more readable, as well as focused on the objectives and novelties of the present manuscript.

REVIEWER #1

Referee comment on "Merging bio-optical data from Biogeochemical-Argo floats and models in marine biogeochemistry" by Elena Terzić, Paolo Lazzari, Emanuele Organelli, Cosimo Solidoro, Stefano Salon, Fabrizio D'Ortenzio, and Pascal Conan

The paper discusses the results of the analysis of ~1300 Biogeochemical ARGO profiles (Temperature, salinity, Chlorophyll fluorescence, downwelling irradiance at three wavelengths and downwelling PAR) generated in different regions of the Mediterranean sea, though covering a large portion of it, by 31 profilers in the years 2012-2016. The analysis is based on the comparison among measured profiles and profiles derived by merging different bio-optical models and 1D biogeochemical simulations based on a 3D coupled biogeochemical model, the OGSTM-BFM (see text for refs). The wide scope motivation is that (P.2 L.22-24): Specific studies are required to demonstrate to what extent the assimilation of radiometric data can improve the model skill in simulating key biogeochemical variables (e.g. nutrients, primary productivity).

R1.1

More specifically the authors want (P.2 L.32-34):

1) to show how it is possible to integrate BGC-Argo float bio-optical data and a simple 1-D model to investigate chlorophyll vertical dynamics; 2) [how] to use such a tool on a sufficiently large data set in order to test different bio-optical models

The text is unclear on a few key issues related to the protocol followed for the simulations (see below). Each simulated profile is generated using the vertical distributions of physical and chemical variables without considering horizontal processes, as the authors write on P.4 L.13-15 ..therefore implying that mass exchanges due to horizontal diffusion and baroclinic components of the (upper ocean) advection field are assumed to be smaller compared to vertical processes and biogeochemical dynamics The impact of this assumption depends on the time scale of integration and on what are the initial conditions of each run, which is not clearly explained.

> The time scale of the simulations corresponds to the typical length of time-series provided by the BGC-Argo float during the period 2012-2016 (11 months on average).
>
> The initial conditions of each simulation, carried out by the OGSTM-BFM coupled physical-biogeochemical model, are provided by the outputs of the reanalyses of the MedBFM model system (composed by the OGSTM-BFM and the 3DVarBio assimilation scheme for surface chlorophyll from satellite, reanalyses released within the Copernicus Marine Environment Monitoring Services) at the corresponding spatial and temporal points of the float deployment. After the initialization, the model evolves without further assimilation of biogeochemical data from the 3D model, and it is not reinitialized. The simulation setup will be more extensively described in the revised version of our manuscript.
>
> We agree with the reviewer that the time scales are important. In particular, we hypothesize that in the experiments considered, several forcings like PAR and mixing are most important on short time scales, whilst other forcings (related to lateral advection of nutrients, for example) act on longer time scales by the modulation of subsurface nutrients inventories. However, we think that an extensive analysis of other mechanisms acting on the horizontal plane or along

isopycnal surfaces interacting with the float trajectory is beyond the scopes of our work. In any case, the analysis of the discrepancies between the 1D model results and the BGC-Argo float data can support the idea that when model and observations significantly disagree, physical and biogeochemical interactions not related to vertical processes may have a substantial role in the representation of the chlorophyll characteristics, not fully resolved by our 1D model framework.

R1.2

A complementary scope is (P.5 L.13-14) ..[to assess] the possibility of using biogeochemical models also when [underwater] PAR measurements are not available, [comparing] the skill of different bio-optical models, which it is generally the rule.

The indicator for testing the performance of the models is the DCM depth, that obtained by the simulations vs. the observed depth, while a minor relevance is given to the DCM amplitude.

The main results of the study are: 1. an assessment of the performance of different formulations and/or parametrizations of the light penetration in the water column in relation to the concentrations of optically active components and 2. that PAR is more important than mixing and nutrients in determining the capability of the model in reproducing in situ chlorophyll profiles.

Indeed, testing different formulations and parametrizations in a model is useful not only to find the best performing model but, more importantly, to analyze the interplay among different mechanisms in generating observed pattern or dynamics.

To better illustrate the effects of the parameterizations on the model indicators, we performed a number of experiments. In the first experiment we partitioned the BGC-Argo floats in couples: each couple is composed by one BGC-Argo float belonging to the western basin and one to the eastern basin, by random selection. Then, for each couple, we switched the initial conditions for nutrients, which allows to estimate the impact on DCM depth. The results are shown in the following scatter plots (Fig. R1):

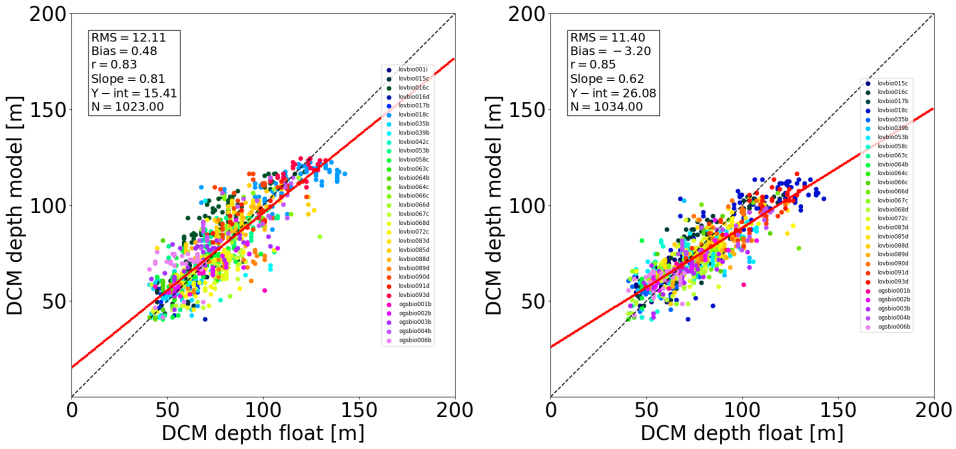

Fig. R1. Scatter plots of DCM depth derived for the REF simulation (left) and with the "East-West" switching technique described in the text (right).

The plots evidence how inverting the initialization of the nutrients does not significantly alter the results in terms of DCM depth. We obtain a reduction of the slope from 0.81 to 0.62, thus it seems that the role of nutrients is secondary compared to light in DCM depth regulation.

Performing the same operation by switching light instead of nutrients is technically more difficult, however, we provided a second experiment to appraise the role of light (and other selected key parameters). This experiment consists in a sensitivity analysis following a similar technique as shown in Huisman et al. (2004). More specifically, we selected two BGC-Argo floats (*lovbio018c* for the east Med and *lovbio067c* for the west Med) and a couple of parameters [Phosphate, Light] and then performed 21x21 simulations (per each float) applying bivariate perturbations. This technique allows to better understand the driving mechanisms for DCM depth variability.

In the revised version of our manuscript, we used such analyses to evaluate the model sensitivity and to add some considerations to the results.

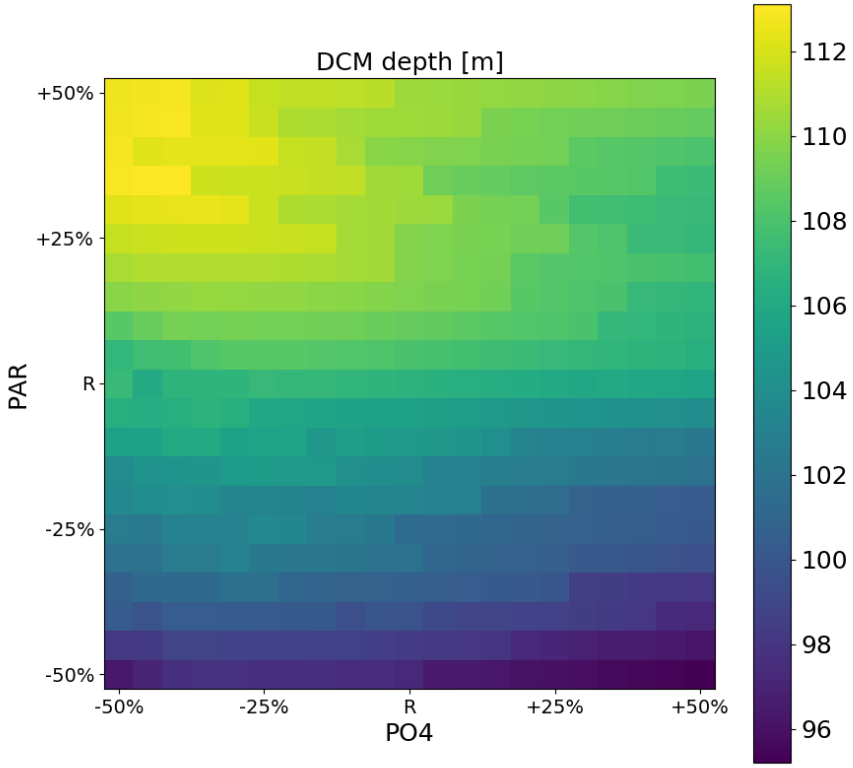

Fig. R2. Sensitivity analysis of DCM depth perturbing *LIGHT* and initial conditions of *PO_4* [both by an uniform factor] along the water column. 'R' marks the reference values. The BGC-Argo float here reported is the *lovbio018c*. Each pixel is a full simulation, for a total of *21x21* simulations. The DCM depth is averaged over the simulation period.

The plot reported in Fig.R2 shows how the DCM position is affected by light and nutrient (PO_4) perturbations. As shown in Fig.R2, perturbing PO_4 of 50% has a minor effect on DCM depth position, whilst perturbing light has a larger impact. Same results hold in the case of the other BGC-Argo float considered (*lovbio067c*). Such experiments were carried out also on additional indicators, such as DCM width and DCM values, as suggested by the other reviewer.

R1.3

This part is often lacking in the discussion. For example the reason why different optical models produce different depths of the DCM varying with the area is not discussed. More important, there is a key conceptual issue in the manuscript, at least from what I could grasp from its present version. The authors compare the chlorophyll vertical profiles, obtained from different bio-optical models and with different values of turbulent diffusivity, with those measured in situ, without discussing the impact on the profile of nutrients, phytoplankton loss due to grazing and all the other processes simulated by the OGSTM-BFM.

We focused on discussing the DCM depth because it is the indicator measured by the BGC-Argo floats that we principally considered in this manuscript. We do not have available synoptic data measured by the BGC-Argo floats (e.g. nutrient concentrations) to corroborate the other outputs produced by the model. Therefore, for variables different from chlorophyll, we can provide at most an evaluation of the impact the bio-optical models have on them. The additional impacts on nutrients and phytoplankton grazing are also driven by the same changes in the parameterizations selected. We assume that on the time scales of the simulation [11 months], the most important mechanisms (light, mixing) are included in the model, thus, the variability of simulated profiles of nutrients should be realistic. As an additional analysis, we perturbed initial conditions of nutrients to evaluate the effect of DCM properties. This allows to explore mechanisms controlling chlorophyll dynamics. Additionally, we perturbed initial condition only for the BGC-Argo floats deployed in the western basin to evaluate the impact on reproducing gradients.

R1.4

I believe that the rationale for this is the assumption that the biogeochemical module is always the same and then any differences in the results would depend only on the change of the specific driver tested. Even ignoring any possible non-linearity in specific processes, e.g., the nitrogen dependence of the photoacclimation by phytoplankton, the best performance of the model in reproducing the depth of the DCM cannot be attributed only to the tested drivers since equally important processes are in the background and not discussed at all, besides some mention to phosphate which is substantiated only by the model outputs. This makes me thinking that the authors consider the 'geochemical' fields produced by the OGSTM-BFM as real data instead than simulated data. This might be a reasonable assumption for large scale patterns but it is a little weaker for daily simulations in single sites that are moved in time. The effectiveness of a bio-optical model should be tested against IOPs or AOPs, as it is already been

done also for BGC-ARGO profilers, not via an end product, i.e., chlorophyll a, whose concentration depend on many other processes. This would also help in clarifying which mechanisms drive the differences reported in Figs. 10 through 12.

We agree with the reviewer and, as suggested, we propose to compare the skill of the models using directly the AOPs, in particular the average irradiance attenuation and the maximum attenuation along the vertical compared to REF that adopts measured values. Considering also the role in nutrients affecting attenuation. Nonetheless, we think that it is important to keep also the comparison with the DCM depth because it is the end product we are mainly interested in the present manuscript.

R1.5

In addition, it not clearly explained, or I might have missed where, if all the state variables simulated by the model were reset each day to the 3D model values for that day and that site, as one might guess from lines 30-33 on P.5 or if, as in a normal 1D simulations, they are produced by the model. In either case I guess some discrepancies should arise, which are neither mentioned nor discussed in the paper.

As explained before, the 1-D model is initialized with the 3-D model only at the first step of the simulation. We mention the fact that neglecting lateral inputs could produce effects that the present methodology cannot replicate. We do not want to stress the dependence on 3-D model configuration because a possible generic application carried out with this approach, e.g. based on the global ocean BGC-Argo float dataset, could be possibly performed independently from any 3D model, and the initialization for nutrients might be based on data available from climatology repositories.

R1.6

While acknowledging the effort invested in the study it looks a bit empirical and I am not convinced that it adds new knowledge to the existing one. Besides solving a couple of issues mentioned in the detailed comments, I suggest to revise the paper analyzing in more detail what are the mechanisms driving the simulated differences and discussing in more detail the extent to which the OGSTM-BFM drives the DCM depth which is the prognostic variable that the author use to test the performance of the different sub-models tested.

We agree to further expand this part in order to make more evident the differences between the REF simulation and the alternative models in terms of skill and formulation. We will add additional indicators in the analysis of REF results (as mentioned in point R2.7).

Detailed comments

Abstract (It should be substantially re-written. Following are some suggestions).

L.3-4 ...Data set comprised of ..Argo Floats does not seem correct. I suggest to rephrase as: The present work is based on a dataset comprised of 1314 0-1000 m vertical profiles of biogeochemical and optical data measured by 31 Biogeochemical (BGC) Argo floats in the Mediterranean Sea from 2012 to 2016. L.4 The data set was integrated in ...sounds a little confusing since the simulations are 1D. I suggest to rephrase as: 1-dimensional model simulations, using measured photosynthetically available radiation (PAR) profiles as light input, were then carried out for each profile along the trajectories of the floats. L.6-7 The simulations were aimed to be consistent with data measured by float sensors, especially in terms of the deep chlorophyll maximum (DCM) depth. I suggest to rephrase as: The simulations were aimed at reproducing the profiles measured by float sensors, especially for what the deep chlorophyll maximum (DCM) depth concerns. L.7-9 I suggest to rephrase as: We tested several light models to estimate their impact on modeled biogeochemical properties taking into account self-shading, derived from vertical chlorophyll distributions, and colored dissolved organic matter (CDOM) concentrations. L.9-11 I suggest to rephrase as: The results, corroborated by the comparison with in- situ BGC-Argo profiles, illustrate how PAR penetration and vertical mixing modulate the dynamics of primary producers along the water column. L.12 Highest? L.13 Simulation results show also that... L.14-15 After reading the paper I am not convinced that The approach here presented serves as a computationally smooth solution to analyse BGC-Argo floats data and to corroborate hypotheses on their spatio-temporal variability.

We agreed to follow the reviewer's suggestions and modified the abstract accordingly

Intro

P.2 L.6 Density? More clear the high number of active BGC-Argos

We reformulated this part.

P.2 L.7 ..numerical experiments of that kind. Unclear. Better: to analyze the predicting capability of bio-optical models, if this is the scope

Ok

P.2 L.19 ones

Ok

P.2 L.6-24 To better clarify the scope of the study it would be better to invert the se- quence of the arguments. If the scope is to: ..to demonstrate to what extent the assimi- lation of radiometric data can improve the model skill in simulating key biogeochemical

variables (e.g. nutrients, primary productivity) which comes as a possible improvement of what already done and sketched before, then this statement should come first. Then all the motivations for using Med data as a test case. If, alternatively, the scope is to improve our understanding of Med functioning then then all the paragraph should be changed accordingly. Reading the manuscript the first possibility seems to hold true.

We reformulated our introduction to make it clearer.

Methods

P.3 L.17 ..were then vertically interpolated to a resolution of 1 m in the upper 400 m. Do the authors mean 'fitted'? If the sampling resolution was 1 m why to interpolate them? What about the data below 250 m? Were they extrapolated?

Yes the data were fitted in order to be regularly spaced as in the case of the model, the data below 250 were extrapolated.

P.3 L.19-21 Could the authors be more explicit on which part of the Baird et al (2016) model they used and with which input variables? This can go in SI.

We will add more details concerning the correction applied to PAR in the supplementary material

P.3 L.21 A second approach. There is no first before.

The corrections we mention are related to the corrections of PAR from planar to scalar, the first is with the formula by Baird et al. (2016), the second is by means of constant correction, we will clarify the text accordingly. For the sake of clarity we left in the text only the selected approach, Baird et al. (2016).

P.3 L.25 please rephrase as: ..measure Chl a concentration using as a proxy its fluorescence emission in the red band (690 nm) after blue excitation at 470 nm (Holm-Hansen et al., 1965)

We changed the text and omitted this part in the updated version.

P.3 l.27 remove it

Ok

P.5 L.20 ..levels

Ok

P.5 L.25 ..characterized regarding..? ..quantified using?

Ok

P.5 L.35 ..allow a gradual increase. . . decrease?

Ok, we can rephrase putting "allowing a vertically smooth transition between mixed and stratified layers."

P.7 eq.1 I might be wrong but as written and with sigma-MLD = 0.3 the first term becomes negligible at the depth of 2 m

The denominator in the argument of the exponential is sigma * MLD, in this way the MLD depth modulates the shape of the mixing profiles in terms of variance of the Gaussian.

P.9 L.5-10 The whole paragraph is a little confusing because the authors introduce the seasonal mixing due to destratification without clarifying that this is likely taken into account by the measured change of the MLD and not by their formulation of mixing (Eq. 1).

The explanation of the formula in Eq.1 should now make the paragraph more clear, in fact, the variance of the Gaussian profile depends on the MLD.

P.10 L.29 remove as

Ok

Fig. 5 The legend could be compacted and the three figures could become one three multipanel figure

Ok, we will try to compact the figure, our only concern is related to readability of the panels if they become too small.

P.18 L.2 are hardly what? Constrained?

Hardly ever in a steady state condition. We mean that the system has time dependent forcing that prevent it to reach the steady state.

P.20 L.23-28 Do the authors implicitly assume that CDOM concentration is higher in the WMed? This could said more explicitly.

Yes, this assumption derives from the preliminary analysis we carried out on Ed 380 BGC-Argo float profiles, for which the Kd 380 were derived. Since the diffusion attenuation coefficient as an apparent optical property depends more on the composition of the examined water body rather than the external light field (i.e. on IOPs), higher Kd values at that wavelength suggest a higher absorption, be it from CDOM and / or non-algal particles (NAP). From the same data set, after an extended analysis, it can be confirmed that a gradient in absorption between west and east Mediterranean is present.

P.27 L.12 The most fitting? May be: The best alternatives to fit the data.

Ok

REVIEWER #2

GENERAL COMMENTS

The authors used a number of vertical profiles from BIO ARGO floats (1314 profiles) in the Mediterranean and merged them with a one dimensional biogeochemical model. The aim of the study was to alter the optical component of the model and study the effect it has on model simulations, specifically on the chlorophyll profile. The authors also showed the effect vertical mixing has on the shape of the chlorophyll profiles. They have demonstrated that bio-optical data from the floats are useful not only for model data comparison, but also as forcing in the model, which in my take is the biggest plus of the work. I complement the authors on their effort combining the data with the model.

The work is well presented and concise. I think the manuscript is well suited to be published in this journal. My suggestion would be to expend some technical aspects, which I outline in more detail with specific comments. These comments are aimed mostly to expand the information in the text.

We thank the reviewer for the encouraging comments, below we reply to the points raised.

SPECIFIC COMMENTS

R2.1

P5 L30 How good is the matchup between the measured chlorophyll profiles and the modeled profiles taken for the initial conditions from the reanalysis?

The following scatter plot (Fig.R3) is equivalent to the one used for the REF model validation but restricted to the initial values taken respectively from reanalyses and the BGC-Argo float data. The number of samples is lower than in the case of the BGC-Argo float results, and therefore difficult to compare with the other scatter plot (Fig.R1). However, we may point out that model tends to overestimate the DCM position (Bias is approximately 7% of the mean DCM depth and the slope is 0.53).

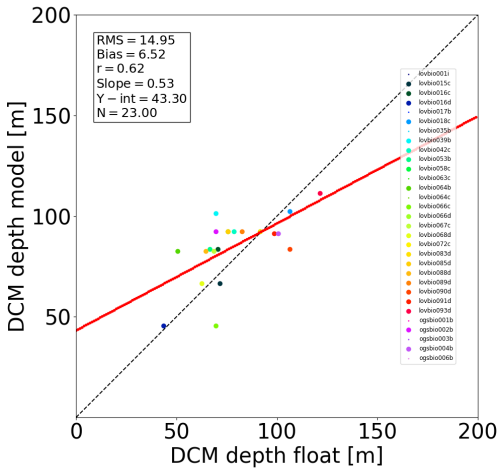

Fig. R3. Same as Fig. R1 (left panel) but only for initial conditions.

R2.2

P5 L22 If I am correct the governing equations for photosynthesis can be found in Lazzari et al. (2012) Appendix B and the remaining equations in Supplementary material of that paper? Please indicate this in more details.

Ok, we propose to add a unambiguous reference: the equations are best summarized in the BFM manual where all the options including the ones used in the present simulation are reported. The supplementary material included in this manuscript contains the biogeochemical parameters that activate the correct options used in the present simulations.

R2.3

P7 Perhaps writing a generic one dimensional equation for the vertical distribution of phytoplankton would be of some help to the non-expert readers of the paper. It would also help to elucidate the mathematical formulations of the various processes which are referred to later on in the text, such as mixing and light attenuation.

We agree with the reviewer. We plan to add the general mathematical equation applied to each tracer:

$$\partial_t C_i(z,t) = \partial_z[D_v(z,t)\partial_z C_i(z,t)] + v_{sink,i}\partial_z C_i(z,t) + BFM_i(T,S,PAR,\overline{C}(z,t))$$

where *Ci* are the biogeochemical tracers simulated (i=1,50), *Dv* is the vertical eddy diffusivity derived from Eq.1 [reported in the first submission of the manuscript]. v_{sink} is the sinking velocity, *BFMi* is the reaction term due to biogeochemical processes for the tracer *Ci*. T, S, PAR are data measured by the BGC-Argo float.

R2.4

P17 Secti 3.2 Some good references for this discussion are: Ryabov & Blasius (2014) The American Naturalist, Huisman et al. (2002) The American Naturalist, Huisman et al. (2004) Ecology, and one with a historical note: Ryabov & Blasius (2008) Mathematical Modelling of Natural Phenomena.

Thank you for the recommendations. We found the literature very helpful and have in turn added these very useful references, in particular to comment the theoretical aspects of the simulated profiles.

R2.5

P7 L19 Does this imply that you have also averaged measured chlorophyll in the 15 m depth intervals along with calculated Kd and then pared them up in the regression? Please clarify.

Yes, we proceeded exactly in this way, which has been specifiedin the revised manuscript.

R2.6

P7 L24 Why are there brackets around ln(Ed)?

The brackets [] are a typo, we will correct it.

R2.7

P9 Figure 2 The depth of the deep chlorophyll maximum is taken as a metric for the model and the model is proven to be very good at predicting the deep chlorophyll maximum depth. However, there are other measures beside this that can be used: surface chlorophyll concentration, chlorophyll concentration at the depth of the maximum and width of the profile. It would be interesting to see this comparison as a scatter plot.

Our initial idea to focus mainly on the shape of the profile was dictated by the complexity of the transformation of fluorescence profiles to chlorophyll concentration values. For this reason, we thought that comparing the simulated DCM depth versus measurements was the most robust action to take. We already included an evaluation of the surface concentration for the stratified period to compare the effect of constant versus diel variation in PAR.

Following the reviewer's suggestions, we show also the DCM width and the DCM magnitude. The DCM width is operationally defined by means of a Gaussian fit and the thickness is computed in the range +/- sigma/2 from the maximum.

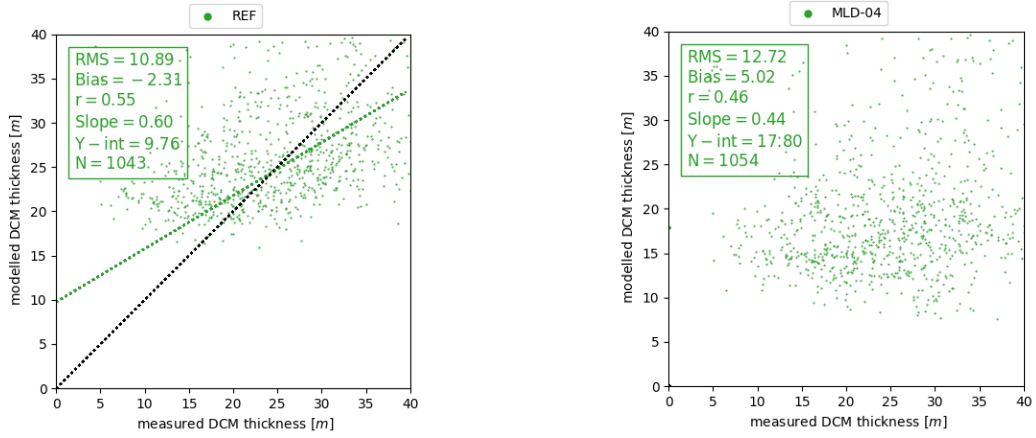

Fig. R4. Scatter plot of DCM thickness as defined in the text. Left panel reports REF simulation ($D_v^{background}=10^{-4}$ m^2s^{-1}), right panel shows MLD04 simulation ($D_v^{background}=10^{-6}$ m^2s^{-1}). The thickness is defined as +/- sigma/2 computed on the vertical profiles by means of a Gaussian fit.

As shown in Fig. R4, the correlation between modeled and measured DCM thickness is lower compared to the DCM depth statistics. The model has a minimum thickness of approximately 15 meters, whereas data reach in some cases 5 meters. As explained in the first version of the paper, background diffusivity regulates the shape of relative maxima. Spatial variability of the background diffusivity coefficient ($D_v^{background}$) in the Mediterranean Sea could be responsible for the higher variability in the DCM thickness observed in data versus model. In the experiments considered as alternative MLD models (MLD01, MLD02, MLD03, MLD04), we changed the $D_v^{background}$ parameter for all BGC-Argo floats for the same amount. The comparison between REF and MLD04 with extreme values of $D_v^{background}$ evidences how, on average, the DCM thickness reduces as diffusivity reduces (Fig. R4, right).

The case of chlorophyll concentration at DCM is more complex. Measured chlorophyll concentration fluctuates in the DCM, and an investigation of the possible underlying mechanisms (e.g. presence of Rossby or Kelvin waves, or other non-linear effects) go beyond the scope of the present paper.

We show here the median chlorophyll in the DCM productive layer (+/- sigma/2) for each BGC-Argo float (Fig.R5). In general, simulations tend to underestimate chlorophyll concentration compared to BGC-Argo floats in the western Mediterranean. In the first version of the manuscript we emphasized how nutrients control the biomass in the DCM productive layer. We evaluated the effects of perturbing nutrients for the BGC-Argo floats deployed in the West Mediterranean by increasing the PO_4 concentration by a factor 2. The results are reported in Fig. R5.

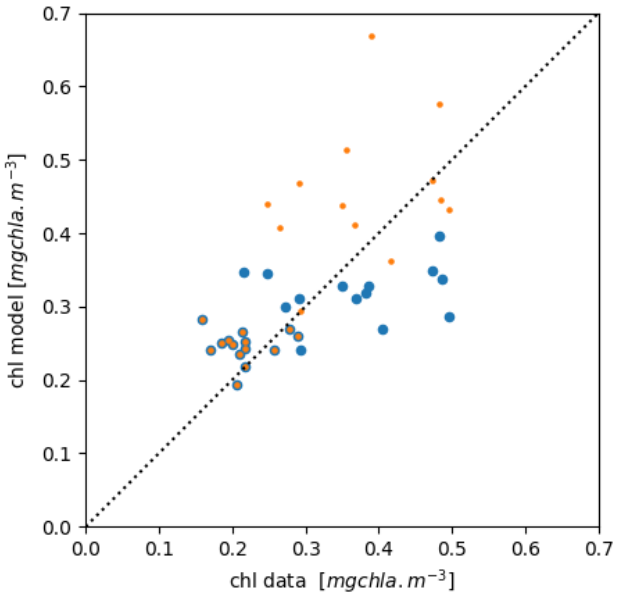

Fig. R5. Scatter plot of DCM chlorophyll concentration as defined in the text: median concentration of the REF (blue dots) and from the simulation increasing PO_4 (orange dots).

The interesting result is that the skill in reproducing the DCM depth, Fig. R1(left), is almost the same between REF and REF with higher PO_4 (image not shown) so it could be possible to finely tune the initial conditions to maximize both the skills in terms of DCM value and DCM depth. But considering the fact that the measurements of concentration of chlorophyll as derived from fluorescence present some uncertainties, we prefer to keep the initialization as based on reanalysis.

For a more detailed overview of the quality control procedure for fluorescence profiles, see Organelli et al. 2017 (**https://www.earth-syst-sci-data.net/9/861/2017/**) as a reference. We will underline this also in the following version of the manuscript.

R2.8

P26 L8 Not quite sure if “irradiance propagation” is a correct term. Light propagates and irradiance is a measure of the light intensity per unit surface. Please change to “irradiance profile”.

Ok, we agree to substitute “irradiance propagation” with “irradiance profile”.

R2.9

P26 L9 Change “position” to “depth”.

Ok.

TECHNICAL CORRECTIONS

I have noticed that in some places units are written with superscript (e.g. m s-1) and in some with a slash (e.g. m/s). Please opt for one to be consistent.

Ok.

Also, in the figures chlorophyll concentration is written with small case letter c as “chl” and in the text it is written with capital letter C as “Chl”. Again, please opt for one to be consistent. I would advise “Chl”.

Ok, we will standardize the notation with Chl.

P6 Table 1 Wrong location of table caption. Should be above the table. P6 Table 2 Wrong location of table caption. Should be above the table. P3 L7 Units are in italics. Please change to upright.P3 L10 Units are in italics. Please change to upright. P7 L7 Mussing full stop at the end of the sentence. P7 L16 Change “BCG-Argo” to “BGC-Argo”.P8 L22 Units are in italics. Please change to upright. P10 L6 Units are in italics. Please change to upright. P10 L18 Missing full stop after “sections”. P17 L9 Remove extra spacing before “where”.P26 L9 Change “what found” to “what was found” or “what has been found”.

Ok, we will apply the corrections listed above.

List of relevant changes in the manuscript:

1. **Abstract** was rewritten
2. **Introduction** was rewritten
3. **Mehods** were revised
4. **Results and discussion** was substantially extended to include a more detailed analysis on the impact of nutrients on model results. To this end the number of simulations performed has been increased significantly. Additionally, comparison of optical model skill not only in terms of chlorophyll but also in term of Kd was included
5. **Conclusions** were expanded including new results and insight derived from the additional simulation performed
6. **Supplementary material** was expanded

In the following part of the document we attach a comparison of the first submitted manuscript with the presently submitted one (R1) processed with latex diff software in order to show the changes performed.

Università degli Studi di Trieste, Dipartimento di Matematica e Geoscienze, Via E. Weiss 2, 34128 Trieste, Italy

Merging bio-optical data from Biogeochemical-Argo floats and models in marine biogeochemistry

Elena Terzić[1,4], Paolo Lazzari[1], Emanuele Organelli[2], Cosimo Solidoro[1], Stefano Salon[1], Fabrizio D'Ortenzio[2], and Pascal Conan[3]

[1]Istituto Nazionale di Oceanografia e di Geofisica Sperimentale - OGS, Via Beirut 4, 34151 Trieste, Italy
[2]Sorbonne Universités, CNRS, Laboratoire d'Océanographie de Villefranche, LOV, F-06230, Villefranche-sur-Mer,France
[3]Sorbonne Université, Pierre et Marie Curie-Paris 06, CNRS - UMR7621 LOMIC, F66650 Banyuls-sur-Mer, France
[4]

Correspondence to: Paolo Lazzari (plazzari@inogs.it)

Abstract. ~~The present work is based on a dataset comprised of 31 Biogeochemical (BGC) Argo floats that collected 0-1000 m vertical profiles of biogeochemical and optical data from 2012 to 2016 in the Mediterranean Sea.The dataset was integrated in 1-dimensional model simulations following the trajectories of each float and considering measured~~ In numerical models for marine biogeochemistry, bio-optical data, such as measurements of the light field, may be important descriptors of the dynamics of primary producers and ultimately of oceanic carbon fluxes. However, the paucity of field observations has limited the integration of bio-optical data in such models so far. New autonomous robotic platforms for observing the ocean, i.e., Biogeochemical-Argo floats, have drastically increased the number of vertical profiles of irradiance, photosynthetically available radiation (PAR) ~~profiles as the reference light parameterization. The simulations were aimed to be consistent with data measured by float sensors, especially in terms of the deep chlorophyll maximum (DCM) depth. Moreover, we tested several light models in order to estimate their impact on modeled biogeochemical properties, including self-shading dynamics based on chlorophyll and colored dissolved organic matter (CDOM) concentrations. The results, evaluated with the corresponding in-situ~~ and algal chlorophyll concentrations around the globe independently of the season. Such data may be therefore a fruitful resource to improve performances of numerical models for marine biogeochemistry. Here we present a work that integrates into a 1-dimensional model 1314 vertical profiles of PAR acquired by 31 BGC-Argo ~~chlorophyll data, indicate that the proposed approach allows to properly simulate the chlorophyll dynamics and illustrate how~~ floats operated in the Mediterranean Sea between 2012 and 2016 to simulate the vertical and temporal variability of algal chlorophyll concentrations. In addition to PAR as input, alternative light and vertical mixing models were considered. We evaluated the models' skill to reproduce the spatial and temporal variability of deep chlorophyll maxima as observed by BGC-Argo floats. The assumptions used to set up the 1-D model are validated by the high number of co-located in-situ measurements. Our results illustrate the key role of PAR and vertical mixing ~~are essential environmental regulation factors driving primary producers dynamics . The higher skills are reached using in-situ PAR, but some of the alternative bio-optical models here presented show comparable skill in reproducing DCM depth spatial variability. Simulation results show that during the stratification phase~~ in shaping the vertical dynamics of

primary produces in the Mediterranean Sea. Moreover, we demonstrate the importance of modeling the diel cycle has significant impact on the surfacechlorophyll regimes. The approach here presented serves as a computationally smooth solution to analyse BGC-Argo floats data and to corroborate hypotheses on their spatio-temporal variability. to simulate chlorophyll concentrations in stratified waters at the surface.

1 Introduction

The availability of radiometric profiles in the open ocean on a global scale has drastically increased due to an enhanced deployment of autonomous Argo floats with additional biogeochemical and optical sensors, officially termed as Biogeochemical-Argo floats (hereafter BGC-Argo floats; Johnson and Claustre, 2016). Their wide use has been also a consequence of refined sensor-calibration and data quality-control procedures that have been applied on acquired profiles (see Organelli et al., 2016, 2017a).

The potential of such observational tools might be further expanded with the upcoming introduction of satellite multi-band sensors (In most biogeochemical models, which are successfully coupled with hydrodynamics, the description of optics is generally (over)simplified, therefore one of the necessary improvements still remains the integration of a more complex optical model, where inherent and apparent optical properties (IOPs and AOPs respectively) are already included as model state variables, (Fujii et al., 2007). The research community is emphasizing the importance of merging different methods in order to improve the skill of numerical models, such as the OLCI sensor on board of assimilation of remote sensing data or the use of in-situ data both for initialization and validation purposes. Until recently, the ESA Sentinel-3 mission[1] and the forthcoming NASA PACE program[1]), as well as in the development, calibration and tuning of use of the latter was especially critical due the scarcity of observations, however the emergence of autonomous robotic platforms such Biogeochemical Argo floats (hereafter BGC-Argo) helped filling the gap in bio-optical numerical models in the ocean (Dutkiewicz et al., 2015; Baird et al., 2016; Gregg and Rous , that can in turn allow a more comprehensive investigation of the link between physical and biogeochemical processes in the oceans.

Due to a high density measurements acquired around the globe regardless of the season.
In particular, the Mediterranean Sea Monitoring and Forecasting Centre (Med-MFC) operatively produces analyses, forecasts and reanalyses of a series of biogeochemical state variables (e.g. chlorophyll, nutrients, pCO2) for the European Copernicus Marine Environment Monitoring Services (CMEMS) since 2015 using the MedBFM model (Lazzari et al., 2010, 2012, 2016) , which assimilates surface chlorophyll from satellite observations (Teruzzi et al., 2014, 2018).
The introduction of BGC-Argo floats and a generally low cloud sky coverage, the Mediterranean Sea represents an ideal location to carry out numerical experiments of that kind. The Mediterranean has clearly been identified as a "hotspot" for climate change, and is therefore expected to experience environmental impacts (de Madron et al., 2011).In addition, has led to a drastic increase in the number of radiometric measurements in the Mediterranean Sea, such as downward irradiance (Ed) and photosynthetically available radiation (PAR), for which specifically developed quality control procedures and refined sensor

[1] https://sentinel.esa.int/web/sentinel/user-guides/sentinel-3-olci
[1] https://pace.gsfc.nasa.gov/

calibration (Organelli et al., 2016, 2017a) have widespread their use (Organelli et al., 2017b; Wojtasiewicz et al., 2018; Gerbi et al., 2016;]
. BGC-Argo can therefore be an important source of high vertical spatial and temporal resolution data that can be integrated in the calibration and tuning of bio-optical numerical models for understanding marine biogeochemistry.

To this end the Mediterranean Sea proves to be an important region to study due to its bio-optically anomalous nature. It is characterized by complex trophic gradients (Crise et al., 1999; Lazzari et al., 2012; d'Ortenzio and Ribera d'Alcalà, 2009) and spatially heterogeneous inherent ~~and apparent~~ optical properties (Oubelkheir et al., 2005). Such gradients are mainly related to the inverse estuarine circulation of the area (Crispi et al., 2001) and to the varying distribution of optically significant substances (e.g. colored dissolved organic matter - CDOM; non-algal particles - NAP) that modulate the light penetration along the water column (Morel and Gentili, 2009b). Moreover, inherent optical properties (IOPs) could be affected also by important processes of Saharan dust deposition (Claustre et al., 2002). ~~Furthermore, the Mediterranean Sea Monitoring and Forecasting Centre (Med-MFC) operatively produces analyses, forecasts and reanalyses of a series of biogeochemical state variables (e.g. chlorophyll , nutrients, pCO2) for the European Copernicus Marine Environment Monitoring Services (CMEMS) since 2015 using the MedBFM model (Lazzari et al., 2010, 2012, 2016), which assimilates surface chlorophyll from satellite observations (Teruzzi et al., 2014). However, it is important to explore the feasibility of the direct assimilation of radiometric quantities that appears~~

At present, no studies have tried to assimilate radiometric quantities into numerical models to improve the simulation of chlorophyll dynamics in this basin and investigate the causes of the vertical, spatial and temporal variability eastward. Assimilating radiometry could prove more robust than ~~the chlorophyll-based one~~ chlorophyll assimilation as a result of a more accurate uncertainty characterization ~~for optical measurements (Dowd et al., 2014; Organelli et al., 2016)~~ of optical measurements (Dowd et al., 2014; Organelli et al., 2016) compared to other ~~properties~~biogeochemical variables, such as fluorescence-derived chlorophyll~~a concentration.~~ .

Specific studies are required to demonstrate to what extent the assimilation of radiometric data can improve the model skill in simulating key biogeochemical variables (e.g. chlorophyll, nutrients, primary productivity).

In this paper we ~~propose a methodology where radiometric quantities measured~~ develop a 1-dimensional model that assimilates PAR profiles acquired by BGC-Argo floats ~~are embedded within a 1-dimensional (1D) numerical model~~ in order to replicate the ~~biogeochemical evolution of the water column observed by floats. For each float a separate simulation is carried out and the measured chlorophyll concentrations(i. e. derived from fluorescence) are compared with the simulated values.~~

~~Given the substantial number of profiles and their high vertical resolution, such simulations can be considered as a convenient evaluation tool of the chlorophyll spatio-temporal patterns along the water column by comparing them with the corresponding in-situ measurements. Furthermore, the present method allows to implement various~~ vertical and temporal dynamics of phytoplankton chlorophyll concentrations. We analyse and validate model performances through a comparison of model outputs with the high number of co-located vertical profiles of chlorophyll concentrations (derived from fluorescence) measured by BGC-Argo floats. Subsequently, we test different mixing and bio-optical models that simulate downward irradiance and evaluate their skills in order to estimate how well they perform compared to in-situ measurements of ~~the photosynthetically active radiation (PAR). The objective of the present study is twofold: 1) to show how it is possible to integrate BGC-Argo float bio-optical data and a~~

simple 1-D model to investigate chlorophyll vertical dynamics; 2) to use such a tool on a sufficiently large data set in order to test different bio-optical models. The PAR. The paper is organized as follows: in the Methods section, the Mediterranean Sea BGC-Argo floats network and the model configurations are presented. In the Results and Discussion section, we analyse the 1D biogeochemical simulations and their sensitivity according to the objectives of the work. General remarks are illustrated in the Conclusions section.

2 Methods

2.1 BGC-Argo floats data

The Mediterranean Sea BGC-Argo network array operating in the period 2012-2016 was composed of 31 floats . The BGC-Argo floats that acquired 1314 vertical profiles, Figure 1, of temperature (T) and salinity (S), chlorophyll *a* concentration (Chl*a*, units of $mg\,m^{-3}$ $\mathrm{mg\,m^{-3}}$), derived from fluorescence measurements between 0 and 1000 m (see Organelli et al., 2017a; Roesler et al., 2017) (see Organelli et al., 2017b; Roesler et al., 2017), and radiometric quantities, such as downward planar irradiance (E_d) at three different wavelengths (λ = 380, 412 and 490 nm, units of $\mu W\,cm^{-2}\,nm^{-1}$ $\mu\,\mathrm{W\,cm^{-2}\,nm^{-1}}$) and Photosynthetically Active Available Radiation (PAR, unit of $\mu mol\,quanta\,m^{-2}\,s^{-1}$) , which gives information on the penetration of light for the whole visible band (from 400 to 700 nm; Kirk, 1994)$\mu\,\mathrm{mol\,quanta\,m^{-2}\,s^{-1}}$) integrated between 400 and 700 nm (Kirk, 1994). Radiometric measurements were obtained in the upper 250 m, with vertical resolution of 1 m between 10 and 250 m and 0.20 m between 0 and 10 m. All profiles were acquired around local noon.

The quality control (QC) procedure for irradiance profiles consisted of dark signal and cloud identification, wave focusing and spikes correction (for a more detailed explanation see Organelli et al., 2016). Chlorophyll concentration QC was performed according to the procedure of the international BGC-Argo program (Schmechtig et al., 2016; Organelli et al., 2017a). The 7 variables (T, S, Chl, of radiometric profiles was specifically designed to identify and remove the dark signal, , , PAR) were then vertically interpolated to a resolution of 1 m in the upper 400 m. atmospheric clouds and wave focusing at the surface (Organelli et al., 2016). Note that the operational definition of PAR used by the BGC-Argo community takes into consideration the planar irradiance E_d rather than the scalar one E_o, therefore differing from its theoretical definition and leading to an underestimation of its values by 30% or more (Mobley et al., 2010). The scalar values of PAR were thus derived according to Baird et al. (2016), although the correction related to the irradiance scattering was neglected due to the lack of information on IOPs . The second approach is based on a constant correction factor: in-situ experiments carried out in the Tyrrhenian Sea indicated that a correction factor of 1.58 can be applied to retrieve scalar from planar irradiance (Dr. Luca Massi, University of Florence, pers. comm.).The two approaches give consistent results with slightly higher skill in the first case, which was adopted in the experiments shown in the following sections.

(see section 1 of supplementary materials).

Vertical profiles of chlorophyll concentration were quality-controlled according to the procedure of the international BGC-Argo float sensors measure Chl *a* concentration through its fluorescent property (Holm-Hansen et al., 1965) of absorbing blue light and re-emitting it at the red part of the spectrum (with the excitation at 470 and emission at 690 nm). The ratio of

~~fluorescence to Chl *a* concentration is highly variable and it depends on the taxonomic composition of the algal species, environmental conditions (temperature and nutrient concentration; Kiefer, 1973), as well on physiological responses to light, such as photoacclimation (MacIntyre et al., 2002; Moore et al., 2006; Falkowski and LaRoche, 1991) and~~ program that removes spikes and corrects for non-zero deep values and non-photochemical quenching ~~(Cullen and Lewis, 1995; Falkowski and Kolber, 1995; Xin~~ ~~. at the surface (Schmechtig et al., 2016; Organelli et al., 2017b).~~ Due to a factory calibration bias ~~in the Chl *a* estimation from fluorescence, a correction~~ for WETLABS ECO series Chl fluorometers, Chl a concentrations were corrected by a factor of 0.5 ~~was applied over the global ocean database for WETLABS ECO series Chl fluorometers after having compared fluorescence-derived values with the ones obtained by high performance liquid chromatography - HPLC (Roesler et al., 2017; Barbieux et a~~

~~A simple geographic partition of profiles was performed with a spatial division~~ (Roesler et al., 2017; Organelli et al., 2017a, b; Barbieux

All the data used in this study are freely available and compiled into the database published by Organelli et al. (2017b). To proceed with our study, 7 variables (T, S, Chl, Ed380, Ed412, Ed490, PAR) were vertically interpolated to a resolution of 1 m in the upper 400 m. Finally, we partitioned the profiles geographically into 13 (out of 16) ~~sub-basins (Fig.~~subbasins (Fig1), with the majority of profiles located in the North Western Mediterranean (NWM, 332 profiles), followed by Northern Ionian (ION3, 172 profiles) and Southern Tyrrhenian (TYR2, 162 profiles). No data were available for the South-western Ionian (ION1) and the Eastern Levantine (LEV4) and only one profile was present in the Northern Adriatic (ADR1), as well as in the Western Levantine (LEV1). The WMO code specification for each BGC Argo float is provided in the section 2 of supplementary material.

2.2 1-D Biogeochemical ~~model~~Model

Biogeochemical processes have been simulated according to the voxel approach ~~("volume element with biological content and processes";~~ ~~, ("volume element with biological content and processes", Kohlmeier and Ebenhöh (2009)),~~ discretized along the vertical in order to resolve vertical irradiance attenuation and nutrient gradients. Each voxel replicated light and mixing conditions according to the trajectory and measurements of the corresponding BGC-Argo float, ~~therefore~~ thus simulating a pseudo-lagrangian experiment. No exchanges of mass between ~~the~~ voxel and the surrounding field have been considered, ~~therefore implying that~~ which implies smaller mass exchanges due to horizontal diffusion and baroclininc components of the (upper ocean) advection field ~~are assumed to be smaller~~ compared to vertical processes and biogeochemical dynamics. Conversely, ~~the~~ voxel exchanges heat with the atmosphere and receives light in accordance with its moving position. ~~This~~ Such an approach, similar to the one ~~already~~ adopted by Kohlmeier and Ebenhöh (2009), has been already successfully applied by Mignot et al. (2018) ~~to analyze~~ in order to analyse BGC-Argo Floats in the North Atlantic.~~Furthermore, we~~

Furthermore, it was assumed that major biogeochemical transformations can be described by the Biogeochemical Flux Model ~~parameterizations (~~(BFM) parametrizations (see below), properly driven by a bio-optical model~~. These assumptions have~~ , which has been validated by contrasting model results and experimental data, as shown later. The model is formulated through

a system of partial differential equations:

$$\partial_t C_i(z,t) = \partial_z[D_v(z,t)\partial_z C_i(z,t)] + v_{sink,i}\partial_z C_i(z,t) + BFM_i(T,S,PAR,\overline{C}(z,t)) \quad (1)$$

where C_i is the i-th biogeochemical tracer simulated (i=1,50), D_v is the vertical eddy diffusivity derived with the vertical mixing model described in subsection 2.2.1, v_{sink} is the sinking velocity and BFM_i is the reaction term corresponding to the tracer C_i. T, S, PAR are the data measured by BGC-Argo floats.

In the first set of simulations, the biogeochemical model was forced ~~by PAR measurements obtained from BGC Argo~~ with PAR from BGC-Argo floats. Experimental values of temperature and density (computed from float ~~temperature and salinity profiles) are~~ profiles) were also taken into consideration.

A simulation for each of the BGC-Argo float trajectories ~~has been~~ was performed with this ~~setup~~set-up, hereafter abbreviated as REF.

Four additional sets of simulations ~~have been performed by using the same setup while considering four~~ were performed on the REF configuration by applying different values of vertical eddy diffusivity coefficients (MLD1, MLD2, MLD3 and MLD4) in order to assess uncertainties ~~in REF simulation due to uncertainties in the vertical diffusion parameterization.After having evaluated the REF model capability, we performed six~~ due to different vertical diffusion parametrization.

Six additional sets of simulations were performed by forcing the biogeochemical model with PAR obtained by alternative bio-optical ~~models~~ parametrizations (OPT1, OPT2a,b,c,d)~~. Moreover, we consider the impact of the bio-optical model approach currently used~~ , one of which considering also the current modeling approach in the CMEMS Copernicus system (OPT3). In this way~~we assessed~~ , the possibility of using biogeochemical models ~~also when PAR measurements are not available, and compared the skill of different bio-optical models.The final~~ in the absence of PAR measurements was assessed.

Finally, a set of simulations ~~has been devoted to explore specific questions, such as~~ was devoted to understand the impact of using a constant light approximation rather than following the diurnal light variation (~~setups~~ CL1 and CL2 ~~). Finally, a first attempt to model the impact of CDOM has been made by adding a new set of variables to both biogeochemical and bio-optical models~~ configurations) on chlorophyll distribution. Furthermore, we evaluated the impact on light propagation due to coloured phytoplankton degradation products, i.e., CDOM, (OPT4a,b,c,d and OPT5). ~~The whole ensemble of simulations is~~ We therefore tested a total of 17 classes of simulations that are summarized in Tab.1 and Tab.2.

The biogeochemical model BFM (Vichi et al., 2013) is a biomass-based numerical model that simulates the biogeochemical fluxes of carbon, phosphorus, nitrogen, silicon, and oxygen, characterizing the lower trophic level (producers, consumers, and recyclers) of the marine ecosystem. ~~Our~~ Its application is based on the coupled transport-biogeochemical model OGSTM-BFM (Lazzari et al., 2012, 2016). ~~The model~~ It includes four phytoplankton functional types (diatoms, nanoflagellates, picophytoplankton, and dinoflagellates), carnivorous and omnivorous mesozooplankton, bacteria, heterotrophic nanoflagellates, and microzooplankton. Each variable is described in terms of internal carbon, phosphorus and nitrogen concentrations. Phytoplankton functional types can be characterized regarding prognostic Chl and can additionally consider the silicate component ~~in the case of~~ for diatoms. Particulate and dissolved organic matter are also included, with the latter partitioned in ~~the~~ labile, semi-labile and semi-refractory phases. The ~~full BFM parameters specification is provided in the supplementary material. Here we focus~~

~~mainly on total Chla~~present study is focused mainly on Chl, reserving to future analysis (according to data availability and optical model complexity) a study of ~~the~~ Plankton Functional Types (PFT) resource competition dynamics ~~and other important aspects of the marine ecosystem.~~

~~In this application, the vertical resolution is 1 meter.~~ (Ryabov and Blasius, 2011, 2014).

Initial conditions for all biogeochemical variables of BFM are provided by the CMEMS reanalysis of Mediterranean Sea biogeochemistry (period 1999-2015, Teruzzi et al., 2014) produced by the MedBFM model system. The initialization profiles are extracted from the MedBFM model output array, taking the nearest model point to the BGC-Argo position in time and space. ~~The vertical profile of~~

Simulations' time scale corresponds to a typical BGC-Argo time-series length during the period 2012-2016, i.e. 11 months on average, with a vertical resolution of 1m. After being initialized, the model evolves without further assimilation of biogeochemical data from the 3D configuration.

Vertical eddy diffusivity coefficient ~~$D_v(z)$ is~~ profiles $D_v(z)$ are here represented as ~~a~~ Gaussian-shaped ~~function~~functions, using potential density values for ~~calculating~~ the mixed layer depth (MLD) calculation with a density-based criterion ~~(D'Ortenzio and Prieur, 2~~ ~~. The Gaussian~~ (de Boyer Montégut et al., 2004; D'Ortenzio and Prieur, 2012). Such a shape is chosen ~~for simplicity~~ due to its simplicity and in order to allow a gradual increase of vertical mixing through the pycnocline. ~~The whole approach and the~~ Approaches and impacts of using different ~~parameterizations to reconstruct the~~ parametrizations to reconstruct mixing along the water column are shown and discussed in section 2.2.1. Since the surfacing of BGC-Argo floats is programmed at around local noon, the variability related to diurnal variation of solar irradiance is ~~accounted~~ taken into consideration according to Kirk (1994).

2.2.1 Vertical Mixing Models

Unlike ~~in the case of~~ radiometric data, ~~we have only access to indirect information on vertical mixing dynamics, which has been~~ vertical mixing is an indirectly obtained quantity, described in terms of potential density ~~obtained~~ (from temperature and salinity data) along the water column. ~~The vertical eddy diffusivity coefficient () is defined as a~~ Vertical eddy diffusivity coefficients (D_v) are defined as Gaussian-shaped ~~function~~ functions in the form of:

$$D_v = D_{vMLD}{}_v^{MLD} e^{-0.5(z/(\sigma\, MLD))^2 - 0.5(\frac{z}{(\sigma * MLD)})^2} + D_{vbackground}{}_v^{background} \quad (2)$$

~~equals 0.3 in all simulations, and~~

σ was identified after ~~initial tuning~~an initial tuning procedure and equals 0.3 in all simulations. Values in REF model are equal to $D_v^{MLD} = 1.0 m^{2s} - 1$ and $D_v^{background} = 10^{-4} m^2 s^{-1}$. ~~The values in the REF model equal and~~

The mixed layer depth (MLD) was defined with the density criterion at the threshold value ~~(D'Ortenzio and Prieur (2012)):~~ (de Boyer Montégut et al., 2004; D'Ortenzio and Prieur, 2012):

$$\Delta\rho_\theta = |\rho_\theta(10m) - \rho_\theta(z)| = 0.03 kg/m^3 kgm^{-3} \quad (3)$$

Table 1. Model configurations considered in the present work. All simulations include diurnal variability except the two cases with continuous light (CL1 and CL2), which use 24-hour averaged irradiance values.

SIM	~~MODELS~~ MODEL DESCRIPTION
REF	~~Reference - E_{dPAR} from Bio-Argo Floats ; $D_{vbackground} = 10^{-4} m^2/s$~~ PAR from BGC-Argo floats ; $D_v^{background} = 10^{-4} m^2 s^{-1}$
CL1	as REF with continuous daily light
CL2	as REF with continuous daily light and ~~$D_{vbackground} = 10^{-6} m^2/s$~~ $D_v^{background} = 10^{-6} m^2 s^{-1}$
MLD1	as REF with ~~$D_{vbackground} = 5\,10^{-5} m^2/s$~~ $D_v^{background} = 5\,10^{-5} m^2 s^{-1}$
MLD2	as REF with ~~$D_{vbackground} = 10^{-5} m^2/s$~~ $D_v^{background} = 10^{-5} m^2 s^{-1}$
MLD3	as REF with ~~$D_{vbackground} = 5\,10^{-6} m^2/s$~~ $D_v^{background} = 5\,10^{-6} m^2 s^{-1}$
MLD4	as REF with ~~$D_{vbackground} = 10^{-6} m^2/s$~~ $D_v^{background} = 10^{-6} m^2 s^{-1}$
OPT1	Riley~~formula: K_{dPAR}~~ : $K_d(PAR)$ = 0.04 + 0.054 ~~$Chl^{2/3}$~~ $Chl^{\frac{2}{3}}$ + 0.0088 Chl
OPT2a OPT2b OPT2c OPT2d	4*$K_d(PAR)$ = a Chl^b + c
OPT3	~~K_{dPAR}~~ $K_d(PAR)$ for the first optical depth ~~z_{opt}~~ z_{od} = ~~z_{eu}~~ z_{eu}/4.6
OPT4a	as OPT2a + Chl degradation to CDOM - time scale 1 day
OPT4b	as OPT2a + Chl degradation to CDOM - time scale 1 week
OPT4c	as OPT2a + Chl degradation to CDOM - time scale 1 month
OPT5	as OPT2a + CDOM following ~~Dutkiewicz et al. (2015)~~ Dutkiewicz et al. (2015)

~~Model configurations considered in the present work, details on the parameters shown in the table are detailed in the text. All simulations include diurnal variability save for the continuous light cases (CL1 and CL2), which use 24-hour averaged irradiance.~~

Table 2. Parameters derived for optical models using BGC Argo float data. For each version of OPT2 only data shallower than z_{max} were used to compute the regression.

~~$K_{dPAR} = a\ Chl^b + c$~~ **Model**	~~z_{max}~~ z_{max}	R^2	**a**	**b**	**c**
OPT2a	150	0.53	0.075 ± 0.0015	0.572 ± 0.018	0.027 ± 0.001
OPT2b	75	0.61	0.064 ± 0.0015	0.615 ± 0.021	0.040 ± 0.002
OPT2c	45	0.71	0.077 ± 0.002	0.469 ± 0.021	0.034 ± 0.002
OPT2d	30	0.75	0.088 ± 0.003	0.406 ± 0.023	0.029 ± 0.003

~~Parameters derived for the optical models using the BGC Argo float data. For each version of OPT2 only data shallower than were used to compute the regression.~~

In ~~the~~ simulations MLD1, MLD2, MLD3, and MLD4, ~~we perturb the $D_{v\ background}$ values~~ $D_v^{background}$ values were perturbed for two orders of magnitude (from 10^{-6} to 10^{-4} ~~m^2/s~~$\mathrm{m^2 s^{-1}}$) in order to estimate the impact ~~that~~ such variations have on ~~the shape of the modeled chlorophyll profile compared to the measured one (see~~ modeled Chl profile shapes compared to measured ones (see Table 1).

2.2.2 Bio-Optical Models

~~In addition to the reference optical model (REF), which is based on radiometric measurements from BGC-Argo floats, several alternative solutions were considered~~Alternative parametrizations to measured PAR profiles were used in models OPT1, OPT2abcd, OPT3, OPT4abc and OPT5. They differ in ~~the method~~ methods used to evaluate the Beer-Lambert attenuation coefficient K_d(PAR), which is parametrized as a function of Chl ~~and/or CDOM~~ concentration rather than being directly calculated from BCG-Argo irradiance data (see Tab.1 and Tab.2).

OPT1 uses the relationship obtained by a statistical analysis done by Riley (1956, 1975):

$$K_{dPARd}(PAR) = 0.04 + 0.0088\,[Chl] + 0.054\,[Chl]^{2/3}\,^{\frac{2}{3}} \tag{4}$$

In ~~model~~ OPT2 ~~we derived a statistical regression between and Chl a~~ models, statistical regressions were carried out between $K_d(PAR)$ and Chl measured by BGC-Argo floats at four different depth ranges: 150 m, 75 m, 45 m and 30 m (OPT2a to OPT2d, see ~~Tab.~~Table 2 for details):

$$K_{dPARd}(PAR) = a + b\,[Chl]^{cb} + c \tag{5}$$

~~with a and b defined as the~~ a and c represent regression coefficients and ~~c as~~ b the exponent (values reported in ~~Tab.2; the confidence~~ Table 2. Confidence intervals were calculated with ~~the~~ Student's two-sided t-test, where the significance level α was set equal to 0.05). ~~The diffuse attenuation coefficient was~~ Diffuse attenuation coefficients $K_d(PAR)$ were calculated for PAR measured by ~~the~~ BGC-Argo floats as the local slope of ~~ln(Ed)~~the natural logarithm of downwelling irradiance for layers of 15 m thickness for the euphotic depth range~~. The euphotic depth~~ , which corresponds to an attenuation of downward planar irradiance to 1% of the subsurface value (Kirk, 1994).

Albeit the regression based on the upper 30 m depth range measurements showed ~~the~~ highest correlation, ~~we considered~~ all four bio-optical models ~~and adopted them~~ were considered and adopted in simulations OPT2a,b,c and d ~~.~~ (Tab.2).

In model OPT3, based on the BGC-Argo data set, $K_d(PAR)$ is calculated for the first optical depth (Morel, 1988), the layer of interest for satellite remote sensing (Gordon and McCluney, 1975), and then adopted as a constant parameter for the entire water column. ~~This kind of description of the diffuse attenuation coefficient~~ Such kind of light extinction definition has been used also in the 3-dimensional version of the OGSTM-BFM model, which integrates $K_d(490)$ data from satellite sensors as the external optical forcing in the ~~Beer-Lambert formulation~~ exponential formulation of downwelling irradiance (for more details see Lazzari et al., 2012, section 2.2.3).

~~The~~ OPT4 and OPT5 models ~~attempt to include the effect of CDOM as it can account for~~ include CDOM dynamics as in the Mediterranean Sea the latter can absorb more than 50% of ~~the light absorption budget in the Mediterranean Sea~~

~~(Organelli et al., 2014; Morel and Gentili, 2009a). In~~ blue light (Organelli et al., 2014; Morel and Gentili, 2009a), thus significantly impacting its attenuation along the water column. OPT4 ~~the assumption is that the degradation of chlorophyll delays the decay of phytoplankton (Organelli et al., 2014) . The attenuation of light~~ assumes that CDOM is correlated to chlorophyll production (Organelli et al., 2014) and that light attenuation is therefore affected by a progressive accumulation of such a constituent ("dead" chlorophyll, initialized at zero concentration)~~and the~~ . In OPT4, accumulation is compensated by ~~a~~ decay (first order kinetic) ~~that is~~ set at different e-folding characteristic times: 1 day (OPT4a), 1 week (OPT4b) and 1 month (OPT4c).~~In~~ OPT5 ~~we used the~~ implemented a formulation of CDOM ~~dynamics~~ as described in Dutkiewicz et al. (2015): a 2% fraction of all ~~the~~ dissolved organic matter (DOM) fluxes is directed to CDOM, including both ~~temperature related~~ temperature-related decay and a photodegradation term based on PAR (Bissett et al., 1999). Additional investigations are provided in section 3.3 to discuss ~~the dynamics of CDOM~~ CDOM dynamics along the water column. Given the mono-spectral ~~formulation presently used~~nature of the current description of light, the attenuation of CDOM on PAR is computed by averaging the exponential law of CDOM absorption (Bricaud et al., 1981) on the visible range.

3 ~~Results and Discussion~~

~~Following the objectives of the paper, we considered~~

2.1 Statistical Analysis

According to the work's objectives, four classes of simulations were considered, which correspond to the following sub-sections: the reference simulation, a subset with perturbed vertical mixing models, ~~a subset of~~ tests with different optical ~~models~~configurations, and a last group of additional ~~tests~~ analyses involving CDOM description and diurnal ~~cycle. The outputs~~ variability. Outputs are validated qualitatively and quantitatively in terms of ~~the~~ profile shapes and the ~~depth of the~~ deep chlorophyll maximum (DCM) depth. The DCM definition is based on the absolute maximum of ~~chlorophyll along depth~~Chl, excluding results of DCM shallower than 40 ~~meters~~ m or deeper than 200 m, as well as the ones with concentrations lower than 0.1 $~~mg/m^3~~\mathrm{mgm}^{-3}$. All results, both for model and BGC-Argo floats, are averaged on a weekly basis. ~~The model outputs are finally~~ Model outputs are compared by means of match-up~~diagrams and~~ , Target and Taylor diagrams (Jolliff et al., 2009). In addition to the DCM depth, the performance in reproducing the DCM thickness and Chl concentration in the DCM layer were also analysed. DCM thickness is operationally defined through a Gaussian fit as $\pm\sigma/2$ from the maximum, thus the Chl concentration at DCM is averaged over the DCM thickness. For a couple of simulations (REF and CL1), skills are also compared at the surface layer (0 - 25 m). In order to avoid corrections due to non-photochemical quenching, profiles acquired only during stratified periods were considered. The target diagram evaluates results with root mean square distance (RMSD) as the main statistical parameter, which was calculated following equation 6:

$$RMSD = \sqrt{\frac{1}{n}\Sigma_{i=1}^{n}\left(m_i - o_i\right)^2} \tag{6}$$

where n is the number of data, m are the model data and o are the observables.

3 Results and Discussion

3.1 Reference Simulation

The assimilation of PAR profiles into the 1-D model helped to accurately estimate the deep chlorophyll maximum depth (Figure 2). The overall model skill in the REF configuration is shown in ~~Fig.2. A good~~ Figure 2, with the histogram within indicating a normal distribution of residuals' deviation. Measured and modelled DCM depth showed high correlation (r=~~0.81~~0.8, p-value <~~0.005)is obtained between DCM depth derived from BGC-Argo floats and the modeled one. The residual plot indicates that the deviation is normally distributed (Fig.2, incut panel). The DCM depth range~~ 0.0005). Both model and measurements indicate that DCM depth varies typically between 50-70 m in western areas (ALB, SWM1, SWM2, NWM, TYR) and is generally deeper in eastern areas (ADR2, ION3, LEV2, LEV3), between 100-140 m. Model tends to slightly underestimate the DCM ~~variability (Fig.~~depth variability (Figure 2, regression slope = ~~0.79~~ 0.81 < 1), in fact, ~~deeper~~ deepest simulated DCM are around 125 m depth, whilst floats data reach 140 m ~~as measured by the lovbio18c BGC float (WMO code 6901528) deployed in the LEV3 subbasin~~(e.g. as shown in Figure 2 lovbio018c data).

~~The chlorophyll patterns present a~~ Chl patterns display high variability both at temporal and vertical scales, ~~Fig.3 to Fig.~~shown in Figures 3 to 6. The subsurface ~~chlorophyll~~ Chl pattern is formed by patchy structures and ~~when fully stratified conditions occur,~~ during stratification periods it is generally deeper moving eastward. BGC-Argo observations indicate that DCM is further eroded by ~~the~~ vertical mixing occurring generally in autumn ~~or~~ and early winter. Simulations provide an adequate reproduction of the ~~timing of the chlorophyll mixing~~ Chl mixing timing and therefore the DCM erosion. ~~The model reproduces also the vertical chlorophyll distribution of the following stratification period (i.e. summer). In fact, if we compare~~ By comparing point-to-point all ~~the Hovmoeller maps (~~Hovmöller maps (considering both depth and time variability) for measured and simulated ~~chlorophyll~~ Chl (examples are reported in ~~Fig.3, Fig.4, Fig.5 , Fig.6)we obtain~~ Figures 3, 4, 5 and 6), a significant average correlation of 0.75 ~~. This confirms quantitatively~~ is obtained: such a result quantitatively confirms that the alternation of mixing and stratification phases, as seen from BGC-Argo chlorophyll measurements, is well reproduced. At surface, the increase in ~~chlorophyll~~ Chl is triggered by rather shallow mixing (0-75 m layer). ~~Overall, results indicate that the discrepancies between the model and dataare higher not only before mixing, but also in the initial phase of the water column re-stratification, hence the transient phases before and after mixing are rather critical to simulate.~~ The initial condition statistics in reproducing DCM depth (R=0.62, slope of 0.53) is improved by the 1-D model for BGC-Argo data.

In addition to ~~the correct timing of~~ a correctly reproduced timing in the alternation of mixing and stratification phases, proved by ~~the good correlation, the simulated chlorophyll also reproduces~~ high correlation, simulated Chl reproduces also episodic signals, such as ~~the deepening of chlorophyll~~ Chl deepening due to specific mixing events. For example, ~~the~~ a mixing event in the NWM ~~sub basin~~subbasin, reaching approximately 200 m depth during winter in 2015, triggers an intrusion of ~~chlorophyll~~

~~(approximately 0.2$mgChl.m^3$) in the~~ Chl (0.2 $\mathrm{mg\,m^{-3}}$) in deeper layers consistently to BGC-Argo float measurements (~~BGC~~ float lovbio067c, ~~Fig.~~Figure 3). Similar dynamics is reproduced in winter 2014 (~~Fig.4) ,~~ Figure 4) for the lovbio035b ~~BGC~~ float drifting from NWM toward ~~ALB sub-basin. Considering the~~ the ALB subbasin.

Considering float trajectories, two kinds of situations are possible: the BGC-Argo float trajectory is relatively stationary in the deployment area (as shown in ~~Fig.~~Figures 3, 5 and 6), or the float passively migrates extensively, following a given water mass (as in ~~Fig.~~Figure 4). It appears that also in the second case, when lateral dynamics effects could ~~be important~~ play an important role in BGC-Argo float measurements, ~~our approach allows to represent the measured chlorophyll patternsadequately~~the approach applied allows an adequate representation of measured Chl patterns. However, it should be noted that in the present multi-float simulation there are no trajectories ~~that include~~ including both west and east Mediterranean basins. In ~~this case~~such cases, strong gradients between deep water nutrient inventories could invalidate the approach, ~~and hence a nudging or a more sophisticated technique could~~ thus nudging or more sophisticated techniques would be required (Kohlmeier and Ebenhöh, 2009). ~~The lateral~~ Lateral advection processes could indeed play an important role, although it appears that in the present case considering data-driven mixing and turbulence effects ~~allows~~ allow to simulate correctly the seasonal variability. The REF simulation can be therefore used as a reference for the following tests on mixing and bio-optical models ~~analyzed in the following sectionsThe results of the REF simulation show~~ analysed in the next sections. Furthermore, REF results demonstrate that irradiance along the water column, besides mixing, is the driving mechanism ~~that controls the~~ controlling DCM depth. ~~As shown in Fig.7a , there is~~ Figure 7a shows a significant correlation between DCM ~~depth and the depth of surface PAR(euphotic depth~~and euphotic depths (i.e. where irradiance reaches 1% of surface PAR), both in ~~the case of the measured Chl and in the simulated one.~~ cases of measured and simulated Chl.

Similar results, valid on annual average conditions, were found by Mignot et al. (2014) in their Eq. 9, where euphotic depth results to be ~~rather than~~ 0.73% rather than 1% of surface PAR~~. But the prevailing interpretation in Mignot et al. (2014) was~~ , interpreting that the DCM is located at a fixed PAR value~~oscillating approximately~~ , oscillating near the 0.5 ~~isolume. Similar~~ $\mathrm{molquanta\,m^{-2}\,day^{-1}}$ isolume. Comparable conclusions can be derived ~~in the present work, Fig. 7b, where we show that same results are valid both in the case of the BGC Argo float and model~~ for analyses presented hereby. Data and model outputs show similar results with a higher variability of critical PAR values in the case of shallower DCM~~. There are exceptions: in Fig.12, which shows the evolution of a BGC-Argo float during a five-week period, the~~ , Figure 7. However, the model-predicted DCM seems strongly constrained by light regime, Figure 12, whilst observed DCM fluctuates up and down over the euphotic depth (see transition from "T=29 weeks" to "T=31 weeks").

In order to further evaluate the dependence of model results on PAR forcing, two numerical experiments were carried out. In the first experiment, BGC-Argo floats were divided in couples composed by one trajectory located in the western basin and the other one in the eastern basin, by random selection. For each couple the initial conditions for nutrients were interchanged, which allows to estimate their impact on DCM depth. Results (see supplementary material, section 4) evidence that the inverted initialization of nutrients does not significantly alter the outcome in terms of DCM depth, resulting in a slope reduction from

0.81 to 0.62, and maintaining similar correlation and bias. Thus it appears that the role of nutrients is secondary compared to the impact of light on DCM depth regulation on such time scales.

Performing the same operation by switching light data instead of nutrients proves to be technically more complex, thus an alternative approach was applied, which consists of a sensitivity analysis similar to the one described in Huisman et al. (2004) . For this purpose, two BGC-Argo floats (lovbio018c and lovbio067c for east and west respectively) and phosphate and PAR parameters were selected, constructing an array of 21x21=441 simulations (per float) for bivariate perturbations. Such technique allows to further understand the driving mechanisms of DCM depth variability.

A perturbation of 50% of the of initial PO_4 condition has only a minor effect on DCM depth position, Figure 8, while changes in light conditions show a large effect (approximately 10 meters difference).

The same sensitivity analysis is used to evaluate model performance in reproducing DCM width and chlorophyll at DCM (plots for both lovbio018c and lovbio067c are included in the supplementary material, section 5). Results indicate that the DCM width has a variability of 6 m in the perturbation range ($\pm 50\%$), as well as that the DCM magnitude is controlled by nutrient availability rather than light. Comparing measured chlorophyll concentrations and model results shows that the skill in reproducing the DCM thickness is lower compared to the DCM depth (Figure 9, r=0.55, slope=0.6).

The DCM thickness varies between 20 and 40 m for the model, whereas a higher variability from 5 m to 40 m is measured by BGC-Argo (Figure 9). In section 3.2 we evidence how DCM thickness is controlled by the background vertical eddy diffusivity coefficient ($D_v^{background}$). 0-25 m average surface chlorophyll shows similar skill (r=0.68, slope=0.63) as in the case of DCM thickness, Figure 10.

The ~~Mediterranean Sea is considered as~~ skill of the 1D model in reproducing DCM magnitude is lower than for the other indicators: measured chlorophyll concentration fluctuates in the DCM and the possible underlying mechanism (e.g. presence of Rossby waves or Kelvin waves) goes beyond the scope of the present paper. We show here the median chlorophyll in the DCM layer ($\pm\sigma/2$) for each BGC-Argo float (Figure 11). In general, simulations tend to underestimate chlorophyll concentration compared to BGC-Argo float in the Western Mediterranean Sea. Following the procedure of the sensitivity analysis shown before, we evaluated the effects of perturbing nutrients for the BGC-Argo floats deployed in the West Mediterranean by increasing them by a factor 2 (orange dots, Figure 11). The skill in reproducing the DCM depth is almost the same between REF and REF with higher nutrients (see supplementary materials section 6), however clearly showing the relevant impact on chlorophyll concentration at DCM. Therefore, it could be possible to finely tune the initial conditions to maximize both skills in terms of DCM value and DCM depth. However, considering the fact that the measurements of concentration of chlorophyll as derived from fluorescence present some uncertainties (Roesler et al., 2017; Barbieux et al., 2018; Organelli et al., 2017a), we prefer to keep the initialization based on reanalysis.

The Mediterranean Sea is a nutrient-limited basin ~~(e.g. Crispi et al., 2001; Lazzari et al., 2016; Powley et al., 2017)~~(e.g. Crispi et al. (200), therefore an insight on the role played by nutrients requires further investigation. Phosphate dynamics ~~evidences how the~~ shows an increase in surface ~~chlorophyll is driven by mixing in the surface layers of nutrients. During the stratification period~~Chl driven by nutrient uptake in upper layers due to convective mixing. During stratification periods, the phospho-cline follows the euphotic layer threshold. From results shown hereby, it ~~appears that beside~~ can be ascertained that together

with a strong correlation between light and ~~the~~ DCM depth, nutrient concentration is an important driver ~~that regulates the~~ in regulating phytoplankton biomass at DCM~~, as depicted in Fig. 13, where the western basin exhibits~~ . Indeed, western subbasins exhibit significantly higher values, ~~both of~~ of both phosphate and biomass, compared to the eastern ~~one.~~ ones, Figure 13. It should be noted that the REF simulation is forced by PAR measurements, hence we evaluate the direct impact of nutrients compared to light on DCM properties. The effect of self-shading by chlorophyll and CDOM can increase the role of nutrients in terms of DCM depth modulation, which can be evaluated only by using bio-optical models where attenuation is regulated by chlorophyll or CDOM as presented in section 3.3.

~~Hovmoeller diagrams of BGC float lovbio067c (WMO code 6901649) comparing measured results and simulated ones (REF). The 6-imaged composite is organized as follows: top row shows PAR, vertical eddy diffusivity and the float trajectory; bottom row shows chlorophyll derived from fluorescence measurements, simulated chlorophyll and simulated phosphate. The thick black-white line indicates the depth where PAR has values of 0.5 (Mignot et al., 2014). The number in parentheses in Model Chl indicates point-point correlation with BGC-Argo float chlorophyll.~~

3.2 Vertical Mixing Models

As shown in the previous section, the vertical distribution of chlorophyll displays a distinct variability, which can be at least partially ascribed to mixing~~(i. e. vertical eddy diffusivity).~~ . Typically, higher vertical eddy diffusivity values imply smoother structures. During the stratification phase, when DCM forms, the controlling mixing parameter is the background diffusivity ~~$D_{v\ \mathrm{background}}$~~ $D_v^{background}$. Simplified theoretical models, such as the KiSS ~~(after the names of: Kierstead and Slobodkin, 1953; Skellam, 195~~ (after the names of Kierstead and Slobodkin (1953); Skellam (1951)), can provide rough quantitative scales in order to determine ~~the~~ minimum vertical length ~~scale~~ scales (L_0) that ~~allows~~ allow formation of stable biomass patches (Ryabov and Blasius, 2008) , including the DCM, in a steady state hypothesis:

$$L_0 \propto \sqrt{\frac{D_v}{\mu}} \tag{7}$$

where D_v is the vertical diffusivity coefficient and μ is the growth rate; in stratified conditions, $D_v = D_v^{background}$. Considering any compact vertical interval with ~~favorable~~ favourable conditions for plankton growth (in terms of irradiance and nutrient availability), the increase of background diffusion over a critical value will produce a dispersal of patchy structures (~~e.g.~~ i.e. a relative maximum of chlorophyll concentration), whereas an increase in growth rate μ can drive the formation of finer scale structures by a reduction of L_0.

The dynamics presented in this study ~~are~~ is much more complex compared to KiSS, both in ~~BGC~~ BGC-Argo floats data and in the 1-D medium-complexity biogeochemical model (BFM). Vertical eddy diffusivity can simultaneously affect nutrients, phytoplankton, and mesozooplankton with intricate interactions~~and feedbacks~~, which in turn make difficult to derive analytical solutions. Moreover, unlike KiSS, both the model and ~~the~~ environment are hardly ever in a steady state condition, as a result of

daily and seasonal oscillations in ~~the~~ physical forcings, which are essentially due to variability in diel irradiance and vertical mixing.

Several simulations, labelled as MLD1, MLD2, MLD3 and MLD4, were carried out by changing the background vertical eddy diffusivity coefficient $D_v^{background}$ values by two orders of magnitude (from ~~to , see Tab.~~$10^{-6}\,\mathrm{m^2\,s^{-1}}$ to $10^{-4}\,\mathrm{m^2\,s^{-1}}$, see Table 1). This subset of simulations (with float-derived PAR) clusters at a correlation of approximately 0.8 with a root mean square difference (RMSD) of DCM depth between 10-15 m. Modeled chlorophyll profiles appear much smoother than the observed ones, following a Gaussian shape for all tested values of eddy diffusivity. Small scale patterns are not detectable even when $D_v^{background}$ values are reduced to a minimum. Further analyses concerning these aspects are shown in section 3.4.

3.3 Bio-Optical Models

The ~~adoption of~~ alternative bio-optical models (OPT1, OPT2, OPT3) ~~results in a correlation reduction~~ were slightly less accurate compared to REF: correlation decreases from 0.8 ~~(of the REF simulation)~~ to 0.6-0.5~~(Fig.14). In particular, ~~, Figure 14. The OPT3 ~~, with almost zero bias , displays~~ simulation showed a bias very close to zero, thus suggesting an intermediate skill compared to assimilated PAR simulations (~~REF and the OPT1 and OP2~~ e.g. REF) and the bio-optical models ~~). In general, the~~ (OPT1 and OPT2). OPT1 and the OPT2 cluster of ~~models~~ simulations show slightly lower correlations with a RMSD of approximately 20 m in all cases, with ~~an increasing~~ increase in bias (almost zero for OPT1 and from 6 m (OPT2a) to -14 m (OPT2d)). ~~This~~ The latter may stem from the fact that ~~the DCM depth~~ statistics performed for ~~the~~ OPT2a to OPT2d models ranged from 150 m to 30 m respectively, therefore lowering the number of ~~points~~ data considered due to a reduced depth interval. Despite an increasing correlation of the bio-optical model linear regression with decreasing depth range, it should be underlined that the equations for lower depth ranges (such as OPT2d for the first 30 m) most likely do not perform well at greater depths, hence a higher bias ~~despite~~ in spite of a higher correlation coefficient~~(, p-value < 0.005).~~.

The ensemble of simulations with alternative optical models shows in all cases smoother curves compared to ~~the measured chlorophyll~~ measured Chl profiles (see ~~Fig.~~Figure 15). ~~The~~ Chlorophyll self-shading effect increases from OPT2a to OPT2d, as explained above, due to ~~the different depth range~~ different depth ranges of the dataset used to compute ~~the bio-optical algorithm regression~~linear regressions. Some of the bio-optical models considered~~in the present work~~, in particular OPT1, OPT2a and OPT2b, ~~appear to be able to~~ reproduce the DCM depth gradient between western and eastern ~~sub-basin~~ subbasins with a tolerance of ~~+/-~~ $\pm$10 ~~meters (Fig.~~m (Figure 16). In ~~the previous publications~~ previous studies (Crispi et al., 2002; Lazzari et al., 2012), the correct simulation of DCM depth longitudinal gradient was obtained by forcing the system with a space-time dependent light attenuation parameter based on ~~a~~ Secchi disk climatology or on satellite ~~Kd490~~ $K_d(490)$ data. Both ~~the~~ empirical approaches prevent to understand whether the origin of such gradients is directly related to ~~the~~ external forcings or, on the contrary, if it can be interpreted as a self-emerging property~~. Here the interpretation of self-emerging property is~~ , i.e. related to the ~~emergence of a feature~~ appearance of features which are not directly and explicitly imposed from the choice ~~in the~~ of boundary conditions or ~~from the choice of the~~ model parameters used ~~for~~ in the numerical experiment (de Mora et al., 2016). Results shown in ~~Fig.16~~Figure 16a suggest that a gradient in DCM depth could be partially reproduced and explained in terms

of internal biogeochemical processes and partially due to external forcings (~~e.g~~ i.e. downward irradiance and nutrient initial conditions), even without considering lateral dynamics.

A direct analysis of the impact of alternative bio-optical models on light attenuation, Figure 16b, indicates that the simulated eastern basin waters present generally lower K_d values (and lower dispersion around the median) for REF and OPT3. In other cases, where self shading is included, the variability is driven by chlorophyll (OPT1, OPT2a, OPT2b, OPT2c, OPT2d and OPT4a, OPT4b, OPT4c) or by chlorophyll and CDOM (OPT5), as bio-optical model parameters do not depend on space and time explicitly. West-east gradients are higher for maximum light attenuation along the water column (cross mark, Figure 16b) where the concentration of chlorophyll is higher. Note that for the OPT3 the average and maximum K_d overlap since K_d is for this simulation constant along the water column.

In fact, the average surface PAR of the dataset ~~we~~ considered is higher in the eastern areas, especially during the months of January (40%), September (15%), October (22%), November (36%), December (16%), probably due to ~~atmospheric weather winter~~ clearer atmospheric weather conditions. During summer, when ~~the~~ DCM stabilizes, the west-east differences in measured surface PAR are lower and ~~they~~ oscillate around 10%, ~~but still they contribute~~ however still contributing in increasing irradiance penetration ~~in~~ at deeper layers. The western and eastern basins are also different in terms of nutrient regimes that in turn impact ~~on~~ biogeochemical dynamics and ~~on~~ the DCM depth gradient in non-trivial ways. In particular, the role of nutrients can be evaluated by perturbing initial conditions for the trajectories starting in the western subbasin, as shown in section 3.1. Results indicate that increased nutrients in the western subbasin cause an amplification of the west-east light attenuation gradients (Figure 16c) related to the increase of chlorophyll.The OPT2a test (with increased nutrients) appears to be the most consistent one compared to REF and OPT3, in terms of Kd west-east gradients.

The emerging conceptual scheme is that the first-order controlling mechanism for DCM depth is related to light propagation along the water column, as shown in REF and OPT3 simulations. Other tests indicate that nutrients modulate K_d consistently with gradients simulated in REF. The temporal scale of subsurface nutrient variability controlling self-shading mechanisms is longer than the one of simulations, suggesting that such a mechanism is especially regulated through initial conditions.

Another key factor pertains ~~the~~ to shorter wavelengths (400-450 nm) in the visible part of the spectrum: when light penetrates deeper along the water column, compounds like CDOM are more effective in absorbing light ~~in the blue spectrum~~ and might in turn enhance spatial gradients in irradiance regimes~~. These factors~~ , which could synergistically contribute to a deeper DCM in ~~the eastern sub-basins. The monospectral formulationof the present model cannot address this aspect, but future model versions equipped with multi-spectral bio-optical models~~ eastern subbasins. However, with a current monospectral formulation, such aspects still cannot be addressed. Multi-spectral configurations linked with specific PFT and CDOM absorption terms ~~(Dutkiewicz et al., 2015) are a fundamental step for further investigations~~are thus needed for future in-depth studies of the questions raised in the present work (Dutkiewicz et al., 2015).

3.4 Daily variable versus constant PAR forcings

The use of daily averaged irradiance (i.e. with continuous light, CL1 and CL2) was compared against ~~simulations that included~~ REF that includes the diurnal variability. A consistent reduction of surface ~~chlorophyll~~ Chl concentrations was observed in

the former case (~~Fig. ??~~Figure 10), with a correlation lower than REF~~)~~, affecting much less (in relative terms) the values around DCM (CL2 is shown in ~~Fig.~~Figure 17). Near the surface, phytoplankton is ~~clearly stressed~~ limited by low nutrients (~~and especially in the eastern part) whereas deeper, near the~~ especially in eastern subbasins) whereas closer to DCM, the trophic limitation is weaker, sometimes null ~~(Behrenfeld and Boss, 2003; Behrenfeld et al., 2004)~~(Behrenfeld and Boss, 2003; Behrenfeld et al., 2004) . One possible explanation could be that ~~the~~ light limitation at ~~the DCM for~~ DCM at a low-irradiance regime is almost linear, thus the averaging effects appear to be having a smaller impact than at ~~the surfacelevels~~surface, where light limitation is highly non-linear due to saturation. Furthermore, the Geider formulation for ~~chlorophyll~~ Chl acclimation (Geider et al., 1998) in ~~the~~ case of diurnal variability generates an increase ~~of the~~ in chlorophyll-to-carbon (Chl:C) ratio. This ~~aspect can have important implications~~ could in turn have important consequences in operational applications, where data assimilation is employed ~~to improve model skill . At~~ for model skill improvement. At the surface, the adoption of a diurnal cycle formulation could reduce ~~the correction~~ corrections made by the assimilation scheme ~~,~~ and therefore minimize possible spurious trends introduced by ~~the assimilation~~ it (Gehlen et al., 2015).

Combining daily-averaged irradiances with lowest diffusivity rates ($D_*^{background}$=$10^{-6}\,\mathrm{m^2\,s^{-1}}$, simulation CL2) results in additional relative chlorophyll maxima at surface layers (see ~~Fig.~~Figure 17, panel "T = 33 weeks"), as well as in increased patchiness of the entire vertical profile. Similar chlorophyll profiles with multiple subsurface maxima were identified in a comprehensive fluorescence data analysis in the Mediterranean Sea, Lavigne et al. (2015). Theoretical consideration predicts different maxima along the water column ~~on the base of the~~ based on Tilman resource competition theory applied to ~~an~~ a heterogeneous system (Ryabov and Blasius, 2011). ~~But presently~~ At this stage, however, it is difficult to assess whether the patchy structures observed in data and model are, for ~~different~~ various reasons, realistic or artefactual. ~~Certainly,~~ Nonetheless, it can be ascertained that the background diffusion needed ~~in the model simulation~~ to maintain such structures in model simulations is very low.

Within the framework of currently used mathematical formulations in the 1-D BFM model, the inclusion of diurnal variability tends to reduce the formation of fine-scaled structures ~~. Therefore, the effects of the diel cycle~~ that could be interpreted in terms of a reduction ~~of~~ in diel growth ~~() or possibly~~ (μ) or seen as a possible perturbation that has an equivalent effect of an increased diffusion.

3.5 Bio optical models with CDOM formulation

~~The~~ OPT4 and OPT5 simulations take into consideration ~~the~~ CDOM dynamics by ~~adding~~ including an additional term ~~to the~~ in OPT2a~~model, where the light attenuation for~~ , where light attenuation by PAR was described only in terms of ~~chlorophyll concentration~~Chl. In OPT4a, b, and c, CDOM is ~~parameterized~~ parametrized as "dead" chlorophyll, by changing only the rate of ~~chlorophyll~~ Chl decay from 1 day to 1 month. ~~This~~ Such simplified dynamics description~~derives by the~~ , albeit arguably, derives from high correlation observed between ~~chlorophyll~~ Chl and CDOM in Morel and Maritorena (2001)~~, although it~~ . It should be noted, however, that no analysis, which could corroborate findings from Morel and Maritorena (2001), was carried out within the dataset examined hereby due to ~~the lack of CDOM concentration data~~a lack of information on CDOM

fluorescence. In all three model configurations, the "dead" chlorophyll accumulation results in higher turbidity levels ~~,~~ that in turn reduce light penetration depths. This is quantified by significantly negative DCM biases (over 40 ~~meters~~ m in OPT04c), which result in shallower DCM compared to BGC-Argo derived profiles ~~. Furthermore, the OPT4 set correlation with floats data is generally lower than 0.6 (Fig.14). As it was indicated in the statistical analysis, the OPT4 group of experiments presents shallower DCM depth~~ since the attenuation of ~~chlorophyll~~ Chl is overestimated even when considering ~~the~~ fastest degradation rates. (Figure 14). The experiment OPT5 mimics the CDOM dynamics described in Dutkiewicz et al. (2015) ~~. A~~ where a lower bias is observed compared to the ~~oversimplified OPT04~~ (over)simplified OPT4 tests (where ~~the correlation coefficients are spanning~~ correlation coefficients range from 0.6 to less than 0.1 for ~~OPT04a to OPT04c~~ OPT4a to OPT4c respectively). OPT5 still results in a negative bias of around 10 m compared to the values from -25 m to -40 m for ~~OPT04a to OPT04c.~~ OPT4a to OPT4c.

In open ocean systems, at least three different mechanisms concerning CDOM entrainment in the euphotic layer are considered: lateral flux of CDOM from terrestrial waters (allochthonous origin), production of CDOM ~~in~~ within the euphotic layer (autochthonous origin) and bottom-up flux of CDOM from the subsurface layer not affected by bleaching (Nelson and Siegel, 2013). ~~Fig.~~

Figure 18 shows an example for a BGC-Argo float deployed in the North West Mediterranean ~~sub-basin~~ subbasin (NWM). The model, ~~despite the~~ regardless of initial conditions, correctly drives CDOM absorption coefficients in deeper layers to low values~~whilst~~ , while an enhanced surface production reinforces mineralization and bleaching and thus realizes a continuum of CDOM reactivity and lability. Results of CDOM variability from the BOUSSOLE site (north-west Mediterranean, Antoine et al. (2008)) show that CDOM absorption ranges to a maximum value of 0.07 m^{-1} and indicate that there is a temporal delay between phytoplankton bloom and a maximum in CDOM absorption ~~(Organelli et al., 2014, fig. 3)~~(Figure 3 in Organelli et al. (2014)), whereas deeper layers (below 100 m) have ~~low~~ generally lower CDOM absorption. The dataset shown in Organelli et al. (2014) evidences that cycles of CDOM accumulation ~~followed~~ are followed by depletion in the upper 10 m due to ~~photo-degradation. In our results the~~ photodegradation in summer. In modeling results presented hereby, bleaching has a deeper effect over ~~all the CDOM 'productive'~~ the entire CDOM "productive" layer (see red and blue lines, ~~Fig.18)and subsurface maxima of CDOM are~~ Figure 18), while the subsurface CDOM maximum is not reproduced. Additional investigations of the OPT5 model configuration can address the ~~dynamics of the autochthonous source and~~ autochthonous source dynamics, as well as the bottom-up flux of CDOM in this region. The lack of CDOM accumulation in deeper layers for the OPT5 configuration hinders a proper analysis of the mechanism suggested in section 3.1 related to the emergence of CDOM from subsurface dark layers. Improving model dynamics calibrations could be possibly achieved by utilizing information on CDOM light absorption from BCG-Argo floats measurements ~~(Xing et al., 2012): this analysis could be potentially useful to understand how much of the CDOM signal is autochthonous and how much allochthonous~~(Xing et al., 2012; Organelli et al., 2017b)
.

4 Conclusions

The coupled ~~1-D~~ modeling/~~BGC-Argo observations~~ experimental approach presented here provides a robust and accurate reproduction of ~~the~~ DCM variability across the Mediterranean Sea. ~~The model~~ Such a combined configuration can integrate in a single framework ~~the~~ multi-data measurements provided by ~~the~~ BGC-Argo floats. DCM is a ubiquitous feature of the ~~chlorophyll~~ Chl vertical structure in the Mediterranean, and different forcing conditions generate geographical gradients in ~~the~~ DCM characteristics (i.e. shallower DCM in ~~the~~ western regions, deepening eastwards). Second-order features, such as impulsive vertical spikes or specific patterns observed in ~~the~~ BGC-Argo profiles, are also qualitatively reproduced. ~~Our results can be summarized as~~ Results for the reference simulation, where measured PAR is adopted, are summarized as follows:

- mixing and irradiance propagation control ~~the chlorophyll~~ Chl dynamics;
- DCM position is mostly controlled by PAR~~, and the present work corroborates what found in Mignot et al. (2014);~~ .
- nutrients control the amount of biomass at DCM.

~~We demonstrate~~ Moreover, it was demonstrated that vertical processes considered in the 1-D model, such as irradiance regimes and vertical mixing, allow to properly reconstruct a large part of ~~chlorophyll~~ Chl dynamics, which was quantified also by ~~the~~ skill diagrams.

The role of nutrients in modulating self-shading (as inferred with bio-optical alternative experiments) appears relevant to shape west-east heterogeneity of vertical light attenuation.

The emerging conceptual scheme is that DCM gradients are directly controlled by irradiance modulation, than is in turn controlled through bio-optical processes which change attenuation according to optically active substances (e.g. chlorophyll, CDOM). Nutrients can impact attenuation by regulating chlorophyll content. The time scale of the nutrient pool variability is longer than the ones considered in the present simulation, thus enabling initial conditions to modulate west-east gradients.

Such kind of data-rich experiments, combined with a 1-D numerical model, could be considered as a useful tool also to a broader community, rather than only to biogeochemical modelers, in particular to address process studies.

~~Moreover, the~~ The presented approach might be useful also to quantify the amount of measured signal related to vertical dynamics and the one derived from other processes, such as horizontal advection and subduction of water masses. The usage of PAR measured from BGC-Argo floats (used in REF, CL1, CL2, MLD1, MLD2, MLD3 and MLD4) provides higher correlations compared to ~~the~~ configurations with alternative bio-optical models (used in OPT1, OPT2, OPT3, OPT4 and OPT5). CL1 (without diurnal cycle) shows overall ~~the~~ highest correlation, comparable with REF (~~Fig.~~Figure 14a).

The comparison of different bio-optical models indicates that, when lacking direct measurements of PAR in ~~the~~ subsurface layers, the most fitting alternatives would be ~~the~~ OPT3, OPT2a and OPT1, that provide ~~a~~ relatively lower bias and higher correlation coefficients (between 0.5 and 0.7), as well as ~~a~~ lower RMSD values compared to REF.

Such an analysis can also suggest the rate of improvement when considering a value of light fully integrated in the visible range of the spectrum (400 to 700 nm, REF) versus simplified approaches (~~e.g.~~ i.e. all the OPT simulations here considered).

These results further support the strategic relevance of BGC-Argo data. Temperature, salinity and radiometric parameters encapsulate fundamental information for the reconstruction of primary producers dynamics and are paramount to investigate hypotheses concerning DCM formation. CDOM fluorescence data measured by BGC-Argo floats could be integrated in ~~the~~ simulations to further infer and reconstruct the observed biogeochemical processes.

Furthermore, considering a general 3-D biogeochemical model, it is not possible to have a full data coverage of the in-water PAR field ~~, therefore the present approach evaluation of bio-optical models skill is useful and the emerging considerations could be~~ without a fully coupled radiative transfer model. Such an approach could be thus exported to more complex 3-D biogeochemical models and generalized ~~to regions other than the Mediterranean Sea (possibly on~~ at a global scale~~)~~.

Code and data availability. The BFM biogeochemical model and its documentation can be downloaded at the following address: http://bfm-community.eu/. The quality-controlled databases used in the present manuscript are publicly available from the SEANOE (SEA scieNtific Open data Edition) publisher at https://doi.org/10.17882/49388 and https://doi.org/10.17882/47142 for vertical profiles and products within the first optical depth, respectively.

Author contributions. E.T. and P.L. have designed the manuscript. E.T. performed the BGC-Argo data analysis, P.L. performed the simulations. All the authors contributed to the manuscript writing.

Competing interests. Authors declare that no competing interests are present.

Acknowledgements. This work is part of the PhD project of Elena Terzić, which was funded under the CMEMS contract for the Biogeochemistry Production Unit for the Mediterranean Sea. The simulations were performed in the framework of the ISCRA C project NOVBIOGE (HP10C8C9O6), granted by CINECA, Italy. This work was supported by the French "Equipement d'avenir" NAOS project (Novel Argo Ocean observing System ~~),~~ - NAOS project funded by Agence Nationale de la Recherche (grant agreement ANR J11R107-F); the "Remotely-sensed biogeochemical cycles of the oceans- remOcean" project funded by the European Research Council (grant agreement 246777); the Argo-Italy project funded by the Italian Ministry of Education, University and Research; and the French Bio-Argo program - Bio-Argo France funded by CNES-TOSCA, LEFE Cyber, and GMMC. We acknowledge sponsorship from the BIOPTIMOD CMEMS Service Evolution project and from the MISTRALS-MERMEX project.

References

Antoine, D., Guevel, P., Desté, J.-F., Bécu, G., Louis, F., Scott, A. J., and Bardey, P.: The "BOUSSOLE" buoy—A new transparent-to-swell taut mooring dedicated to marine optics: Design, tests, and performance at sea, Journal of Atmospheric and Oceanic Technology, 25, 968–989, 2008.

Baird, M. E., Cherukuru, N., Jones, E., Margvelashvili, N., Mongin, M., Oubelkheir, K., Ralph, P. J., Rizwi, F., Robson, B. J., Schroeder, T., et al.: Remote-sensing reflectance and true colour produced by a coupled hydrodynamic, optical, sediment, biogeochemical model of the Great Barrier Reef, Australia: comparison with satellite data, Environmental Modelling & Software, 78, 79–96, 2016.

Barbieux, M., Uitz, J., Bricaud, A., Organelli, E., Poteau, A., Schmechtig, C., Gentili, B., Obolensky, G., Leymarie, E., Penkerc'h, C., et al.: Assessing the Variability in the Relationship Between the Particulate Backscattering Coefficient and the Chlorophyll a Concentration From a Global Biogeochemical-Argo Database, Journal of Geophysical Research: Oceans, 123, 1229–1250, 2018.

Behrenfeld, M. J. and Boss, E.: The beam attenuation to chlorophyll ratio: an optical index of phytoplankton physiology in the surface ocean?, Deep Sea Research Part I: Oceanographic Research Papers, 50, 1537–1549, 2003.

Behrenfeld, M. J., Prasil, O., Babin, M., and Bruyant, F.: In search of a physiological basis for covariations in light-limited and light-saturated photosynthesis, Journal of Phycology, 40, 4–25, 2004.

Bissett, W., Walsh, J., Dieterle, D., and Carder, K.: Carbon cycling in the upper waters of the Sargasso Sea: I. Numerical simulation of differential carbon and nitrogen fluxes, Deep Sea Research Part I: Oceanographic Research Papers, 46, 205–269, 1999.

Bricaud, A., Morel, A., and Prieur, L.: Absorption by dissolved organic matter of the sea (yellow substance) in the UV and visible domains 1, Limnology and oceanography, 26, 43–53, 1981.

Claustre, H., Morel, A., Hooker, S., Babin, M., Antoine, D., Oubelkheir, K., Bricaud, A., Leblanc, K., Queguiner, B., and Maritorena, S.: Is desert dust making oligotrophic waters greener?, Geophysical Research Letters, 29, 2002.

Crise, A., Allen, J., Baretta, J., Crispi, G., Mosetti, R., and Solidoro, C.: The Mediterranean pelagic ecosystem response to physical forcing, Progress in Oceanography, 44, 219–243, 1999.

Crispi, G., Mosetti, R., Solidoro, C., and Crise, A.: Nutrients cycling in Mediterranean basins: the role of the biological pump in the trophic regime, Ecological Modelling, 138, 101–114, 2001.

Crispi, G., Crise, A., and Solidoro, C.: Coupled Mediterranean ecomodel of the phosphorus and nitrogen cycles, Journal of Marine Systems, 33, 497–521, 2002.

Cullen, J. J. and Lewis, M. R.: Biological processes and optical measurements near the sea surface: Some issues relevant to remote sensing, Journal of Geophysical Research: Oceans, 100, 13 255–13 266, 1995.

de Boyer Montégut, C., Madec, G., Fischer, A. S., Lazar, A., and Iudicone, D.: Mixed layer depth over the global ocean: An examination of profile data and a profile-based climatology, Journal of Geophysical Research: Oceans, 109, 2004.

de Madron, X. D., Guieu, C., Sempere, R., Conan, P., Cossa, D., D'Ortenzio, F., Estournel, C., Gazeau, F., Rabouille, C., Stemmann, L., et al.: Marine ecosystems' responses to climatic and anthropogenic forcings in the Mediterranean, Progress in Oceanography, 91, 97–166, 2011.

de Mora, L., Butenschön, M., and Allen, J. I.: The assessment of a global marine ecosystem model on the basis of emergent properties and ecosystem function: a case study with ERSEM, Geoscientific Model Development, 9, 59–76, doi:10.5194/gmd-9-59-2016, https://www.geosci-model-dev.net/9/59/2016/, 2016.

d'Ortenzio, F. and Ribera d'Alcalà, M.: On the trophic regimes of the Mediterranean Sea: a satellite analysis, Biogeosciences, 6, 139–148, 2009.

Dowd, M., Jones, E., and Parslow, J.: A statistical overview and perspectives on data assimilation for marine biogeochemical models, Environmetrics, 25, 203–213, 2014.

Dutkiewicz, S., Hickman, A. E., Jahn, O., Gregg, W. W., Mouw, C. B., and Follows, M. J.: Capturing optically important constituents and properties in a marine biogeochemical and ecosystem model, Biogeosciences, 12, 4447–4481, doi:10.5194/bg-12-4447-2015, https://www.biogeosciences.net/12/4447/2015/, 2015.

D'Ortenzio, F. and Prieur, L.: The upper mixed layer, Life in the Mediterranean Sea: A look at habitat changes, edited by: Noga Stambler, Nova Science Publisher, pp. 127–156, 2012.

Falkowski, P. and Kolber, Z.: Variations in chlorophyll fluorescence yields in phytoplankton in the world oceans, Functional Plant Biology, 22, 341–355, 1995.

Falkowski, P. G. and LaRoche, J.: Acclimation to spectral irradiance in algae, Journal of Phycology, 27, 8–14, 1991.

Falkowski, P. G. and Raven, J. A.: Aquatic photosynthesis, Princeton University Press, 2013.

Fujii, M., Boss, E., and Chai, F.: The value of adding optics to ecosystem models: a case study, Biogeosciences Discussions, 4, 1585–1631, 2007.

Gehlen, M., Barciela, R., Bertino, L., Brasseur, P., Butenschön, M., Chai, F., Crise, A., Drillet, Y., Ford, D., Lavoie, D., Lehodey, P., Perruche, C., Samuelsen, A., and Simon, E.: Building the capacity for forecasting marine biogeochemistry and ecosystems: recent advances and future developments, Journal of Operational Oceanography, 8, s168–s187, doi:10.1080/1755876X.2015.1022350, https://doi.org/10.1080/1755876X.2015.1022350, 2015.

Geider, R. J., Maclntyre, H. L., and Kana, T. M.: A dynamic regulatory model of phytoplanktonic acclimation to light, nutrients, and temperature, Limnology and oceanography, 43, 679–694, 1998.

Gerbi, G. P., Boss, E., Werdell, P. J., Proctor, C. W., Haëntjens, N., Lewis, M. R., Brown, K., Sorrentino, D., Zaneveld, J. R. V., Barnard, A. H., et al.: Validation of ocean color remote sensing reflectance using autonomous floats, Journal of Atmospheric and Oceanic Technology, 33, 2331–2352, 2016.

Gordon, H. R. and McCluney, W.: Estimation of the depth of sunlight penetration in the sea for remote sensing, Applied optics, 14, 413–416, 1975.

Gregg, W. W. and Rousseaux, C. S.: Simulating pace global ocean radiances, Frontiers in Marine Science, 4, 60, 2017.

Holm-Hansen, O., Lorenzen, C. J., Holmes, R. W., and Strickland, J. D.: Fluorometric determination of chlorophyll, Journal du Conseil, 30, 3–15, 1965.

Huisman, J., Sharples, J., Stroom, J. M., Visser, P. M., Kardinaal, W. E. A., Verspagen, J. M., and Sommeijer, B.: Changes in turbulent mixing shift competition for light between phytoplankton species, Ecology, 85, 2960–2970, 2004.

Johnson, K. and Claustre, H.: Bringing biogeochemistry into the Argo age, Eos, 97, 2016.

Jolliff, J. K., Kindle, J. C., Shulman, I., Penta, B., Friedrichs, M. A., Helber, R., and Arnone, R. A.: Summary diagrams for coupled hydrodynamic-ecosystem model skill assessment, Journal of Marine Systems, 76, 64–82, 2009.

Kiefer, D.: Fluorescence properties of natural phytoplankton populations, Marine Biology, 22, 263–269, 1973.

Kierstead, H. and Slobodkin, L.: The size of water masses containing phytoplankton blooms, Journal of Marine Research, 38, 1953.

Kirk, J. T.: Light and photosynthesis in aquatic ecosystems, Cambridge university press, 1994.

Kohlmeier, C. and Ebenhöh, W.: Modelling the biogeochemistry of a tidal flat ecosystem with EcoTiM, Ocean dynamics, 59, 393–415, 2009.

Lavigne, H., D'Ortenzio, F., Ribera D'Alcalà, M., Claustre, H., Sauzède, R., and Gacic, M.: On the vertical distribution of the chlorophyll a concentration in the Mediterranean Sea: a basin-scale and seasonal approach, Biogeosciences, 12, 5021–5039, doi:10.5194/bg-12-5021-2015, https://www.biogeosciences.net/12/5021/2015/, 2015.

Lazzari, P., Teruzzi, A., Salon, S., Campagna, S., Calonaci, C., Colella, S., Tonani, M., and Crise, A.: Pre-operational short-term forecasts for Mediterranean Sea biogeochemistry, Ocean Science, 6, 25–39, 2010.

Lazzari, P., Solidoro, C., Ibello, V., Salon, S., Teruzzi, A., Béranger, K., Colella, S., and Crise, A.: Seasonal and inter-annual variability of plankton chlorophyll and primary production in the Mediterranean Sea: a modelling approach, Biogeosciences, 9, 217, 2012.

Lazzari, P., Solidoro, C., Salon, S., and Bolzon, G.: Spatial variability of phosphate and nitrate in the Mediterranean Sea: A modeling approach, Deep Sea Research Part I: Oceanographic Research Papers, 108, 39–52, 2016.

Leymarie, E., Penkerc'h, C., Vellucci, V., Lerebourg, C., Antoine, D., Boss, E., Lewis, M. R., D'Ortenzio, F., and Claustre, H.: ProVal: A new autonomous profiling float for high quality radiometric measurements, Frontiers in Marine Science, 5, 437, 2018.

MacIntyre, H. L., Kana, T. M., Anning, T., and Geider, R. J.: Photoacclimation of photosynthesis irradiance response curves and photosynthetic pigments in microalgae and cyanobacteria1, Journal of phycology, 38, 17–38, 2002.

Mignot, A., Claustre, H., Uitz, J., Poteau, A., D'Ortenzio, F., and Xing, X.: Understanding the seasonal dynamics of phytoplankton biomass and the deep chlorophyll maximum in oligotrophic environments: A Bio-Argo float investigation, Global Biogeochemical Cycles, 28, 856–876, 2014.

Mignot, A., Ferrari, R., and Claustre, H.: Floats with bio-optical sensors reveal what processes trigger the North Atlantic bloom, Nature communications, 9, 190, 2018.

Mobley, C., Boss, E., and Roesler, C.: Ocean optics web book, 2010.

Moore, C. M., Suggett, D. J., Hickman, A. E., Kim, Y.-N., Tweddle, J. F., Sharples, J., Geider, R. J., and Holligan, P. M.: Phytoplankton photoacclimation and photoadaptation in response to environmental gradients in a shelf sea, Limnology and Oceanography, 51, 936–949, 2006.

Morel, A.: Optical modeling of the upper ocean in relation to its biogenous matter content(Case I waters), Journal of Geophysical Research, 93, 749–10, 1988.

Morel, A. and Gentili, B.: The dissolved yellow substance and the shades of blue in the Mediterranean Sea., Biogeosciences, 6, 2009a.

Morel, A. and Gentili, B.: A simple band ratio technique to quantify the colored dissolved and detrital organic material from ocean color remotely sensed data, Remote Sensing of Environment, 113, 998–1011, 2009b.

Morel, A. and Maritorena, S.: Bio-optical properties of oceanic waters- A reappraisal, Journal of Geophysical research, 106, 7163–7180, 2001.

Nelson, N. B. and Siegel, D. A.: The global distribution and dynamics of chromophoric dissolved organic matter, Annual Review of Marine Science, 5, 447–476, 2013.

Organelli, E., Bricaud, A., Antoine, D., and Matsuoka, A.: Seasonal dynamics of light absorption by chromophoric dissolved organic matter (CDOM) in the NW Mediterranean Sea (BOUSSOLE site), Deep Sea Research Part I: Oceanographic Research Papers, 91, 72–85, 2014.

Organelli, E., Claustre, H., Bricaud, A., Schmechtig, C., Poteau, A., Xing, X., Prieur, L., D'Ortenzio, F., Dall'Olmo, G., and Vellucci, V.: A Novel Near-Real-Time Quality-Control Procedure for Radiometric Profiles Measured by Bio-Argo Floats: Protocols and Performances, Journal of Atmospheric and Oceanic Technology, 33, 937–951, 2016.

Organelli, E., Barbieux, M., Claustre, H., Schmechtig, C., Poteau, A., Bricaud, A., Boss, E., Briggs, N., Dall'Olmo, G., D'Ortenzio, F., et al.: Two databases derived from BGC-Argo float measurements for marine biogeochemical and bio-optical applications, Earth System Science Data, 9, 861, 2017a.

Organelli, E., Claustre, H., Bricaud, A., Barbieux, M., Uitz, J., D'Ortenzio, F., and Dall'Olmo, G.: Bio-optical anomalies in the world's oceans: An investigation on the diffuse attenuation coefficients for downward irradiance derived from Biogeochemical Argo float measurements, Journal of Geophysical Research: Oceans, 2017b.

Oubelkheir, K., Claustre, H., Sciandra, A., and Babin, M.: Bio-optical and biogeochemical properties of different trophic regimes in oceanic waters, Limnology and oceanography, 50, 1795–1809, 2005.

Powley, H. R., Krom, M. D., and Van Cappellen, P.: Understanding the unique biogeochemistry of the Mediterranean Sea: Insights from a coupled phosphorus and nitrogen model, Global Biogeochemical Cycles, 2017.

Riley, G. A.: Oceanography of Long Island Sound, 1952-54, vol. 15, Bingham Oceanographic Laboratory, 1956.

Riley, G. A.: Transparency-chlorophyll relations, Limnology and Oceanography, 20, 150–152, 1975.

Roesler, C., Uitz, J., Claustre, H., Boss, E., Xing, X., Organelli, E., Briggs, N., Bricaud, A., Schmechtig, C., Poteau, A., et al.: Recommendations for obtaining unbiased chlorophyll estimates from in situ chlorophyll fluorometers: A global analysis of WET Labs ECO sensors, Limnology and Oceanography: Methods, 2017.

Ryabov, A. and Blasius, B.: Population growth and persistence in a heterogeneous environment: the role of diffusion and advection, Mathematical Modelling of Natural Phenomena, 3, 42–86, 2008.

Ryabov, A. B. and Blasius, B.: A graphical theory of competition on spatial resource gradients, Ecology Letters, 14, 220–228, 2011.

Ryabov, A. B. and Blasius, B.: Depth of the biomass maximum affects the rules of resource competition in a water column, The American Naturalist, 184, E132–E146, 2014.

Schmechtig, C., Poteau, A., Claustre, H., D'Ortenzio, F., Dall'Olmo, G., and Boss, E.: Processing Bio-Argo particle backscattering at the DAC level, 2016.

Skellam, J. G.: Random dispersal in theoretical populations, Biometrika, 38, 196–218, 1951.

Teruzzi, A., Dobricic, S., Solidoro, C., and Cossarini, G.: A 3-D variational assimilation scheme in coupled transport-biogeochemical models: Forecast of Mediterranean biogeochemical properties, Journal of Geophysical Research: Oceans, 119, 200–217, 2014.

Teruzzi, A., Bolzon, G., Salon, S., Lazzari, P., Solidoro, C., and Cossarini, G.: Assimilation of coastal and open sea biogeochemical data to improve phytoplankton simulation in the Mediterranean Sea, Ocean Modelling, 132, 46 – 60, doi:https://doi.org/10.1016/j.ocemod.2018.09.007, http://www.sciencedirect.com/science/article/pii/S1463500318303184, 2018.

Vichi, M., Cossarini, G., Gutierrez, M., Lazzari, P., Lovato, T., Mattia, G., Masina, S., McKiver, W., Pinardi, N., Solidoro, C., and Zavatarelli, M.: The Biogeochemical Flux Model (BFM): Equation Description and User Manual, BFM Report series 1, BFM version 5 (BFM-V5), Bologna, Italy, http://bfm-community.eu, 2013.

Wojtasiewicz, B., Hardman-Mountford, N. J., Antoine, D., Dufois, F., Slawinski, D., and Trull, T. W.: Use of bio-optical profiling float data in validation of ocean colour satellite products in a remote ocean region, Remote Sensing of Environment, 209, 275–290, 2018.

Xing, X., Morel, A., Claustre, H., Antoine, D., D'Ortenzio, F., Poteau, A., and Mignot, A.: Combined processing and mutual interpretation of radiometry and fluorimetry from autonomous profiling Bio-Argo floats: Chlorophyll a retrieval, Journal of Geophysical Research: Oceans, 116, 2011.

Xing, X., Morel, A., Claustre, H., D'Ortenzio, F., and Poteau, A.: Combined processing and mutual interpretation of radiometry and fluorometry from autonomous profiling Bio-Argo floats: 2. Colored dissolved organic matter absorption retrieval, Journal of Geophysical Research: Oceans, 117, 2012.

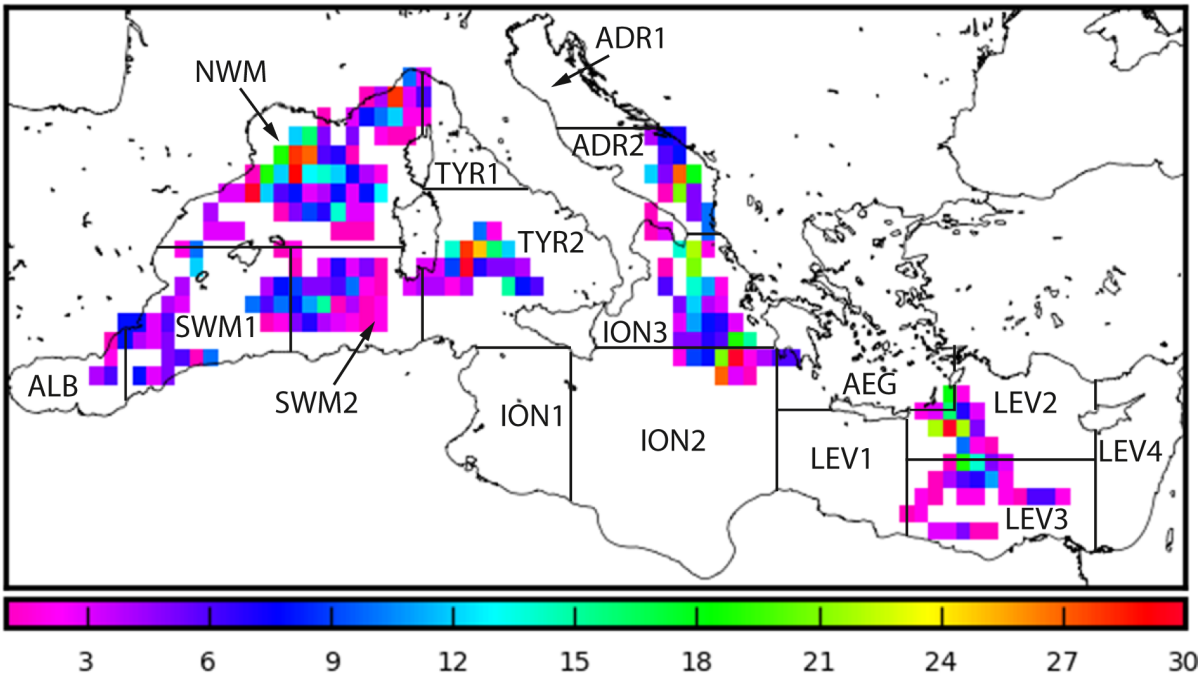

Figure 1. Spatial distribution of BGC-Argo float profiles superimposed to ~~sub-basin~~ subbasin division used in the Mediterranean Copernicus Marine Environment Monitoring Service (CMEMS) system~~.~~

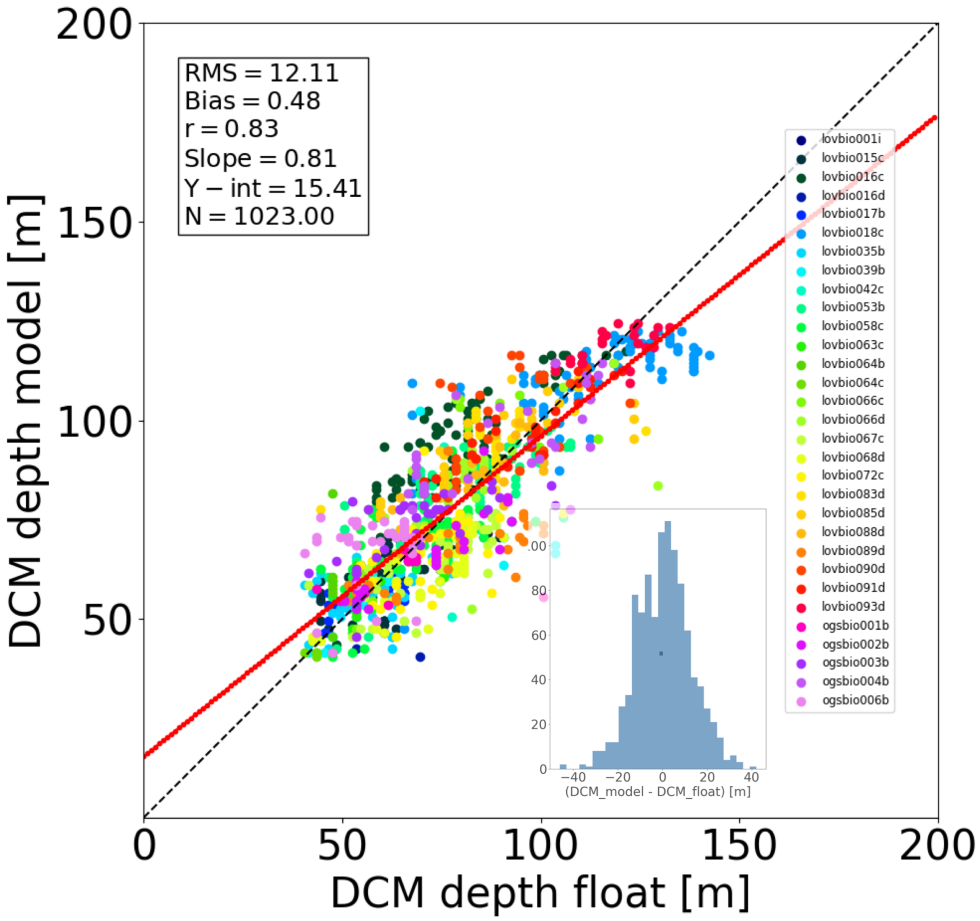

Figure 2. Match-up diagram comparing ~~the depth of~~ DCM depth obtained from BGC-Argo floats data versus REF model results. Each dot corresponds to a weekly profile. ~~DCM depth definition is detailed in text.~~ The red line ~~is~~ depicts the linear regression ~~of the~~ between data ~~versus~~ and model values, defined by its slope and intercept (Y-int~~reported~~) shown in the box. ~~RMS~~Units of RMSD, Bias and Y-int ~~reported in the top left box~~ are in meters. The correlation ~~r~~ coefficient r is significant, ~~p-value~~with p-value < 0.005. The ~~incut figure~~ bottom sub-figure shows the ~~histogram of the~~ residuals' histogram.

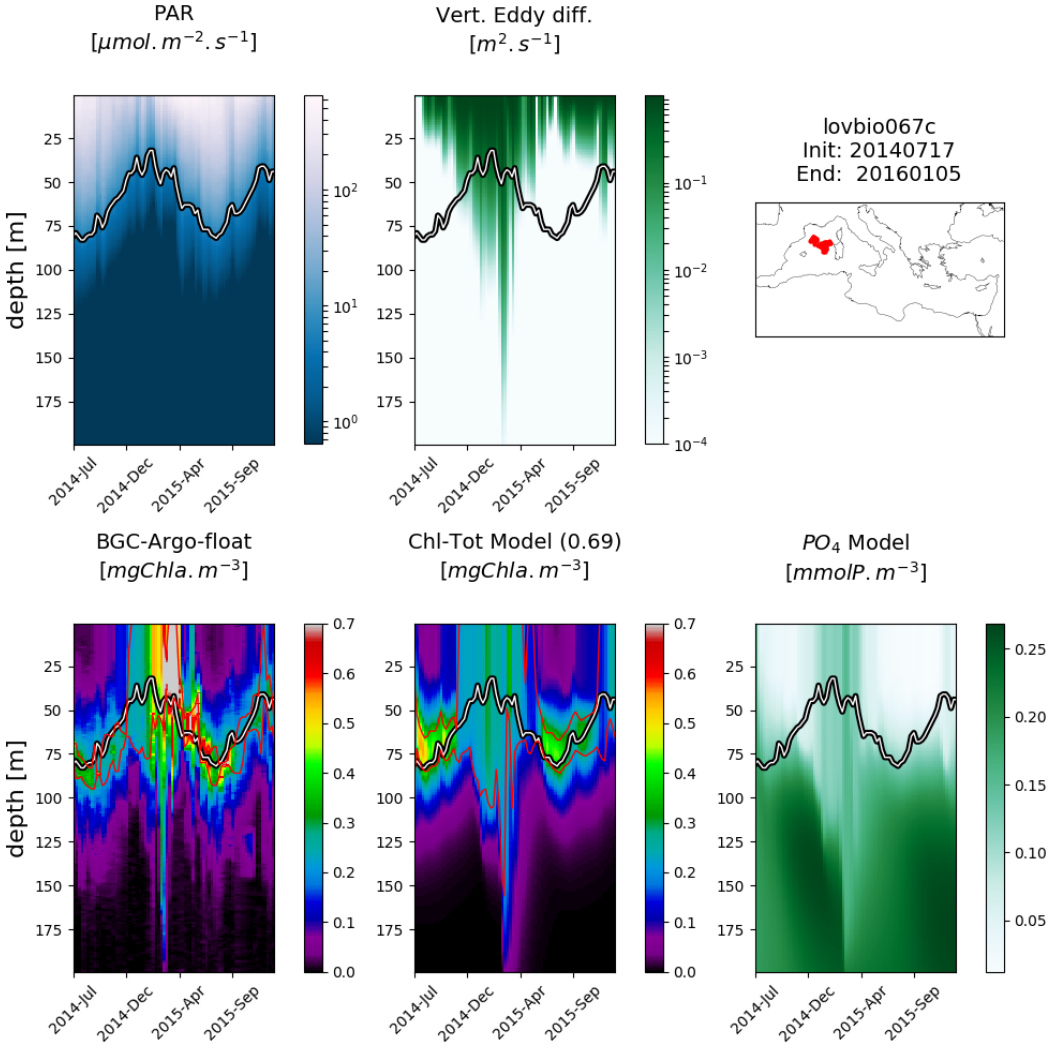

Figure 3. Hovmöller diagrams of BGC-Argo float lovbio067c (WMO code 6901649) comparing measured results and simulated ones (REF). The 6-imaged composite is organized as follows: top row shows PAR, vertical eddy diffusivity and the float trajectory; bottom row shows Chl derived from fluorescence measurements, simulated Chl and phosphate. The thick black-white line indicates the depth where PAR equals 0.5 $\mathrm{molquanta\,m^{-2}\,day^{-1}}$ (Mignot et al., 2014). The number in parentheses in modelled Chl indicates point-by-point correlation with BGC-Argo float Chl.

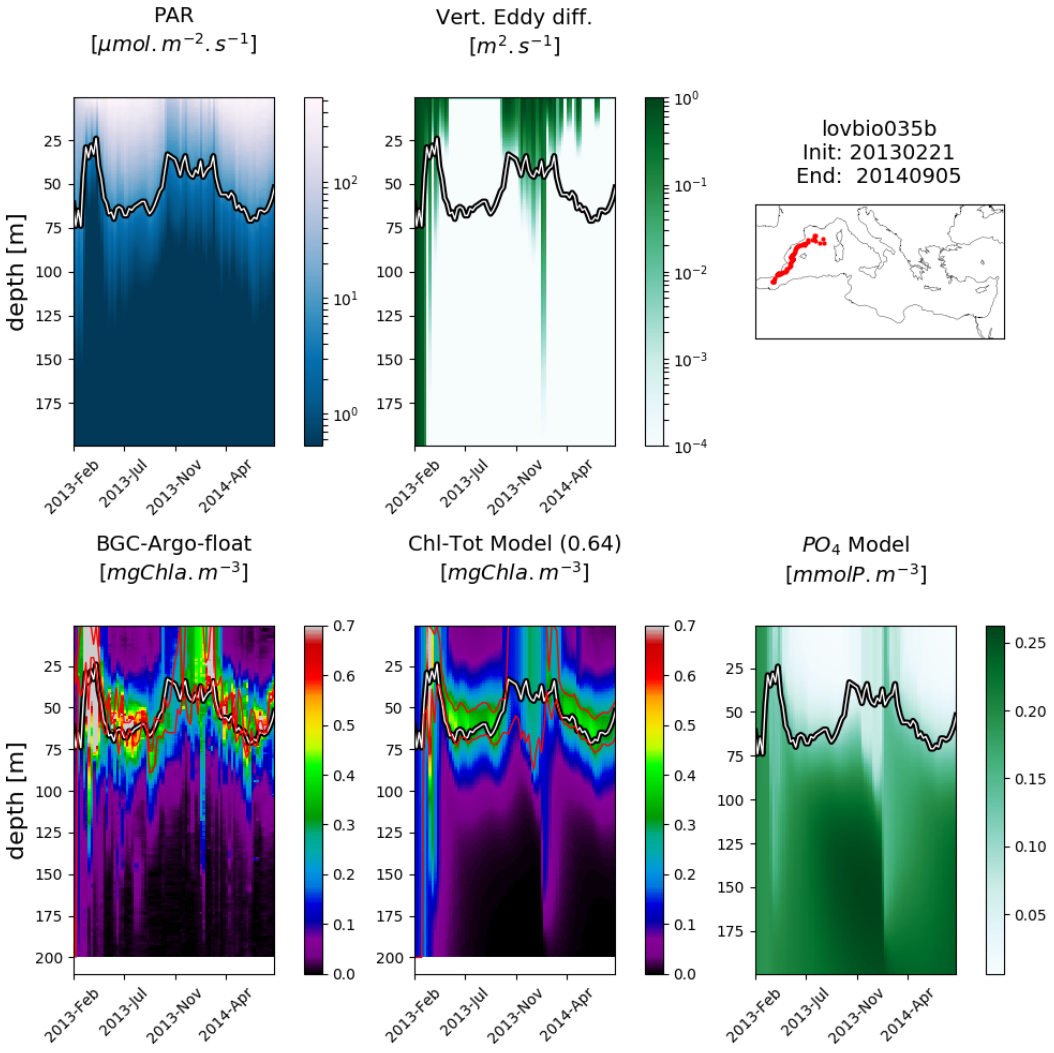

Figure 4. As Figure 3 but for the BGC-Argo float lovbio035b (WMO code 6901511).

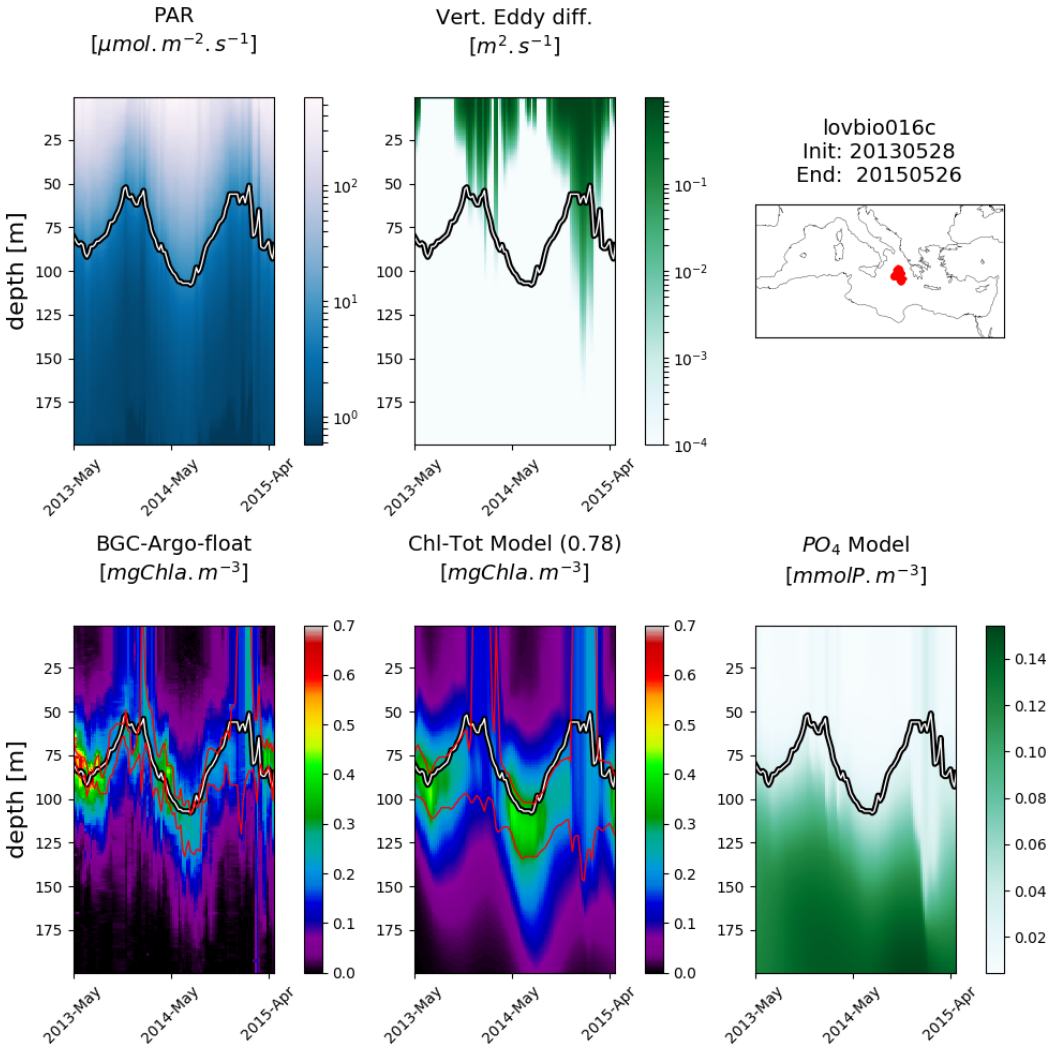

Figure 5. As Figure 3 but for BGC-Argo float lovbio016c (WMO code 6901510).

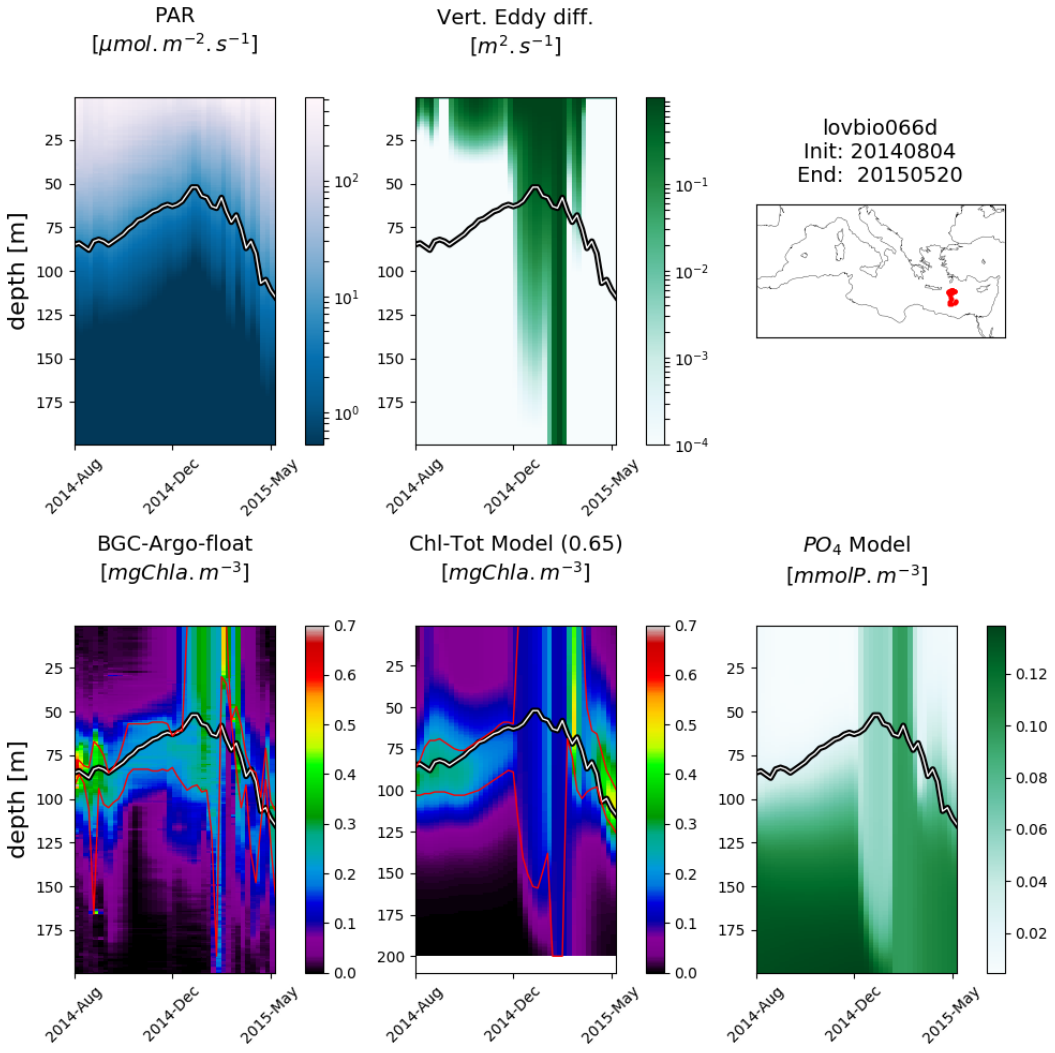

Figure 6. As Figure 3 but for BGC-Argo float lovbio066d (WMO code 6901655).

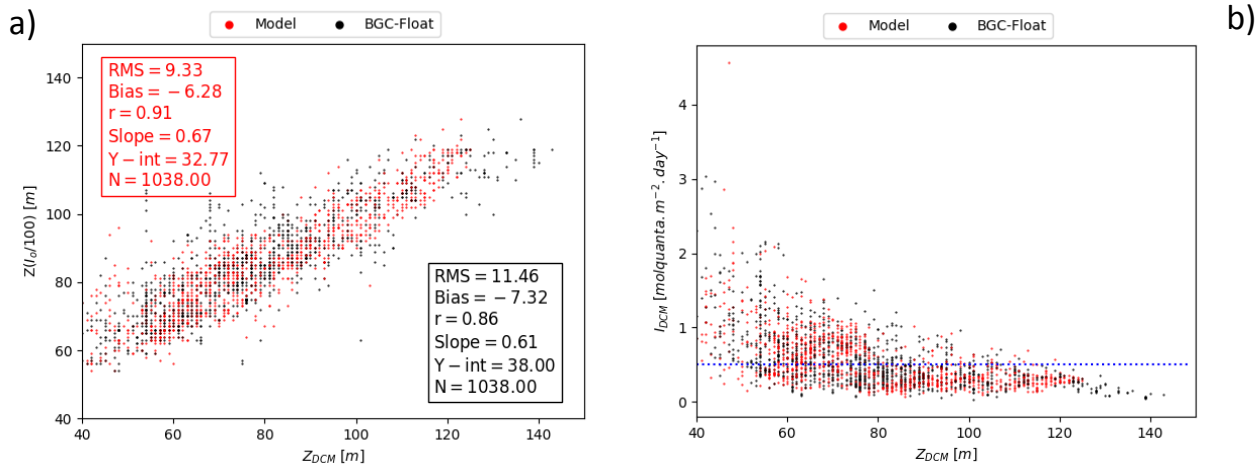

Figure 7. Panel a) DCM depth (z_{DCM}, x-axis) compared to the euphotic depth (z_{eu}, y-axis) both for modelled (red dot) and measured results (black dot). Red box (top left) reports statics for model z_{DCM} versus z_{eu}, whereas the black box (bottom right) shows statistics for z_{DCM} derived from chlorophyll data versus z_{eu}. Panel b) irradiance values (y-axis) at DCM depth (x-axis) both for modelled (red dot) and measured results (black dot). Horizontal blue line marks the 0.5 irradiance threshold (units $\mathrm{molquanta\,m^{-2}\,day^{-1}}$) as identified in Mignot et al. (2014).

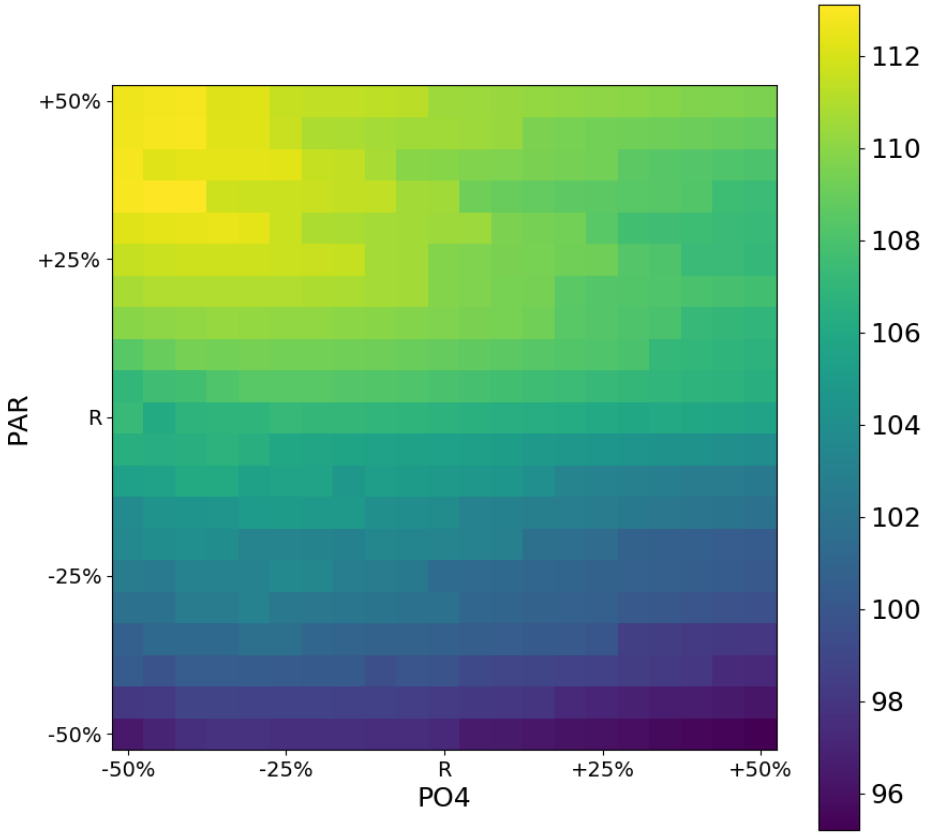

Figure 8. Sensitivity analysis of DCM depth perturbing light and initial conditions of PO4 (both by an uniform factor reported on axis in percentage) along the water column. 'R' marks the reference values. The BGC-Argo float here reported is the lovbio018c. Each pixel is a full simulation of a total of 21x21 simulations. The DCM depth is averaged over the simulation period.

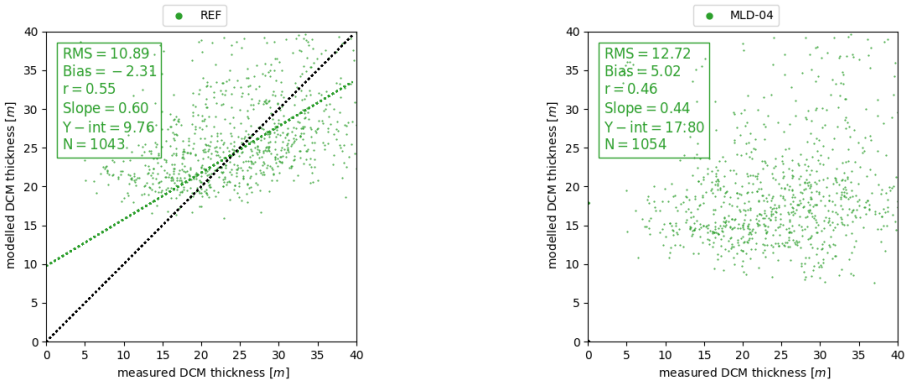

Figure 9. Scatter plot of DCM thickness. Left panel reports REF simulation ($D_v^{background}$ =$10^{-4}\mathrm{m}^2\mathrm{s}^{-1}$), right panel shows MLD04 simulation ($D_v^{background}$ =$10^{-6}\mathrm{m}^2\mathrm{s}^{-1}$). The thickness is defined as $\pm\sigma/2$ centered on the maximum computed on the vertical profiles by means of a Gaussian fit.

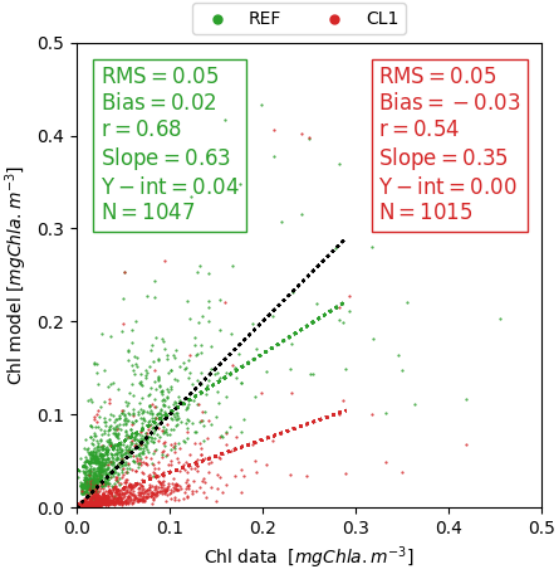

Figure 10. Scatter plot comparing 0-25 m average surface chlorophyll versus BGC-Argo float data for the stratified period condition (DCM > 40 m).

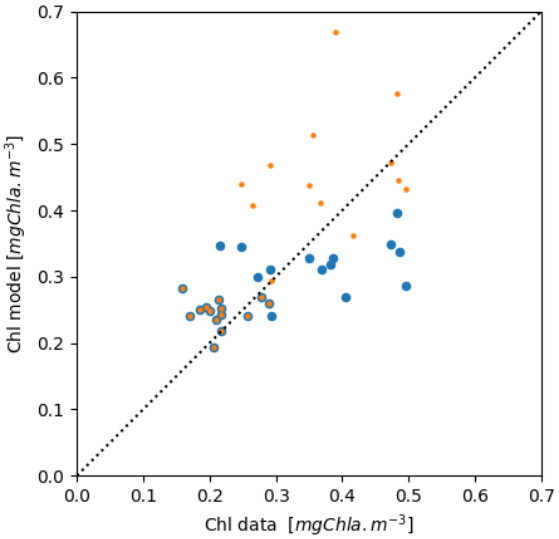

Figure 11. Scatter plot of DCM chlorophyll concentration as defined in the text: median concentration of the REF (blue dots) and from the simulation increasing PO4 (orange dots).

~~Hovmoeller diagrams of BGC float lovbio035b (WMO code 6901511) comparing measured results and simulated ones (REF). The 6-imaged composite is organized as follows: top row shows PAR, vertical eddy diffusivity and the float trajectory; bottom row shows chlorophyll derived from fluorescence measurements, simulated chlorophyll and simulated phosphate. The thick black-white line indicates the depth where PAR has values of 0.5 (Mignot et al., 2014). The number in parentheses in Model Chl indicates point-point correlation with BGC-Argo float chlorophyll.~~

~~Hovmoeller diagrams of BGC float lovbio016c (WMO code 6901510) comparing measured results and simulated ones (REF). The 6-imaged composite is organized as follows: top row shows PAR, vertical eddy diffusivity and the float trajectory; bottom row shows chlorophyll derived from fluorescence measurements, simulated chlorophyll and simulated phosphate. The thick black-white line indicates the depth where PAR has values of 0.5 (Mignot et al., 2014). The number in parentheses in Model Chl indicates point-point correlation with BGC-Argo float chlorophyll.~~

~~Hovmoeller diagrams of BGC float lovvio066d (WMO code 6901655) comparing measured results and simulated ones (REF). The 6-imaged composite is organized as follows: top row shows PAR, vertical eddy diffusivity and the float trajectory; bottom row shows chlorophyll derived from fluorescence measurements, simulated chlorophyll and simulated phosphate. The thick black-white line in the PAR panels indicates the depth where PAR has values of 0.5 (Mignot et al., 2014). The number in parentheses in Model Chl indicates point-point correlation with BGC-Argo float chlorophyll.~~

~~Panel a) DCM depth (, x-axis) compared to the euphotic depth (, y-axis) both for model results (red dot) and measured results (black dot). Red box (top left) reports statics for model ZDCM versus Zeu, whereas the black box (bottom right) shows statistics for derived from chlorophyll data versus . Panel b) Irradiance values (y-axis) at DCM depth (x-axis) both for model results (red dot) and measured results (black dot). Horizontal blue line marks the 0.5 irradiance threshold (units) as identified in Mignot et al. (2014).~~

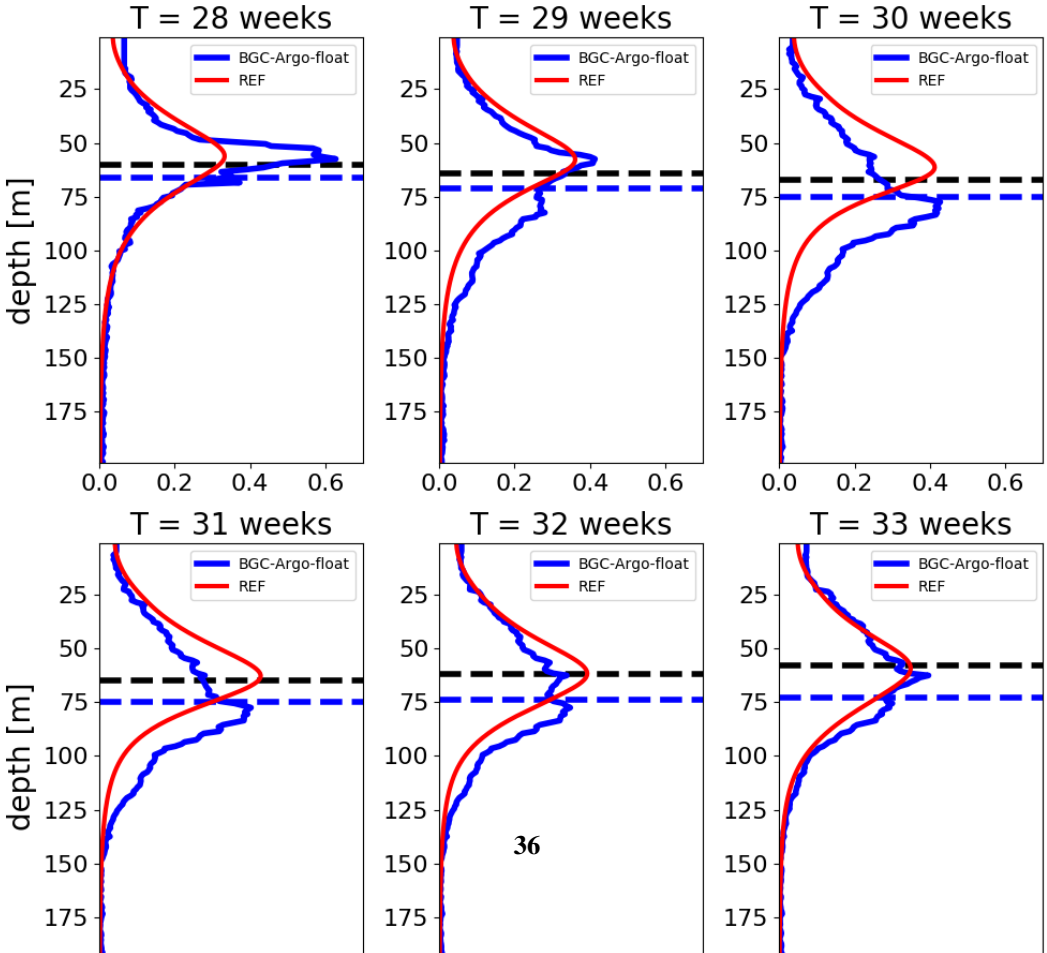

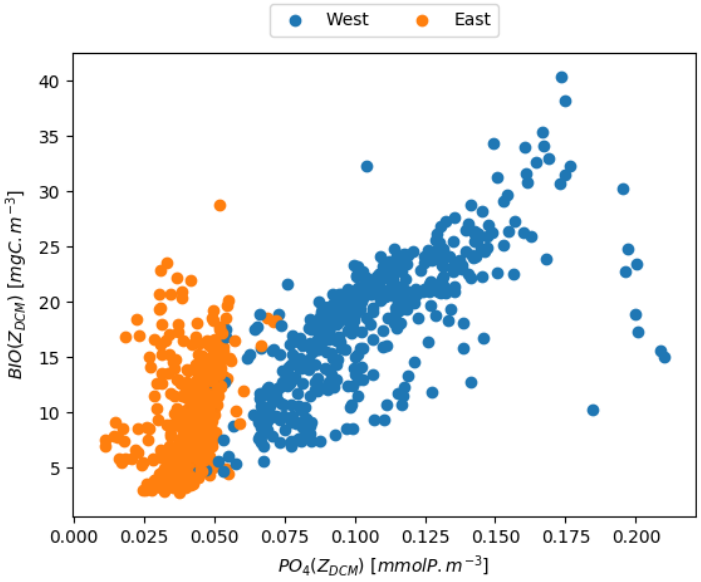

Figure 13. Phosphate ~~concentration~~ (x-axis) and total biomass concentration (y-axis) of phytoplankton at DCM depth~~. All the~~ , including all modeled ~~BGC~~ float trajectories~~are included~~.

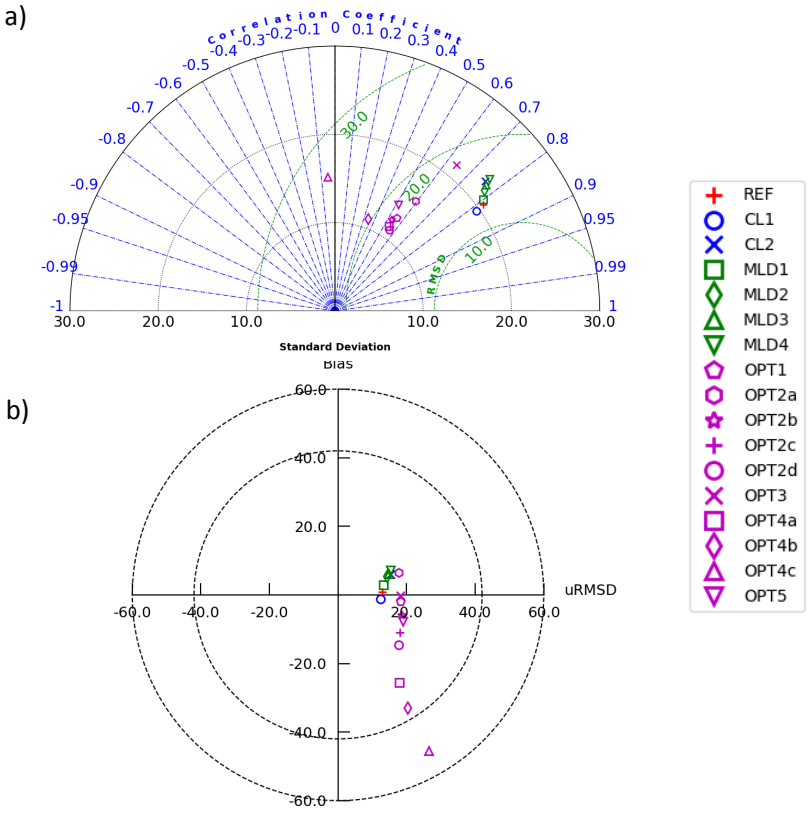

Figure 14. Panel a): Taylor diagram showing ~~the~~ model skill in reproducing DCM depth ~~as~~ compared to data. Correlation is represented by the angle with positive x axis, whereas ~~the distance~~ distances from the origin ~~depicts the~~ depict standard ~~deviation~~deviations. Green circles illustrate iso-contours of RMSD levels. Panel b): Target diagram showing ~~the~~ model skill in reproducing DCM depth compared to data. Distance to the origin ~~is~~ defines the RMSD, all units are in meters. The position on ~~the x axis~~ x-axis is positive if the model standard deviation ~~in the model~~ is higher than the one from data results and negative in the opposite situation. For the sake of completeness, all ~~the model~~ models considered are reported in these ~~summary~~ summarizing skill diagrams.

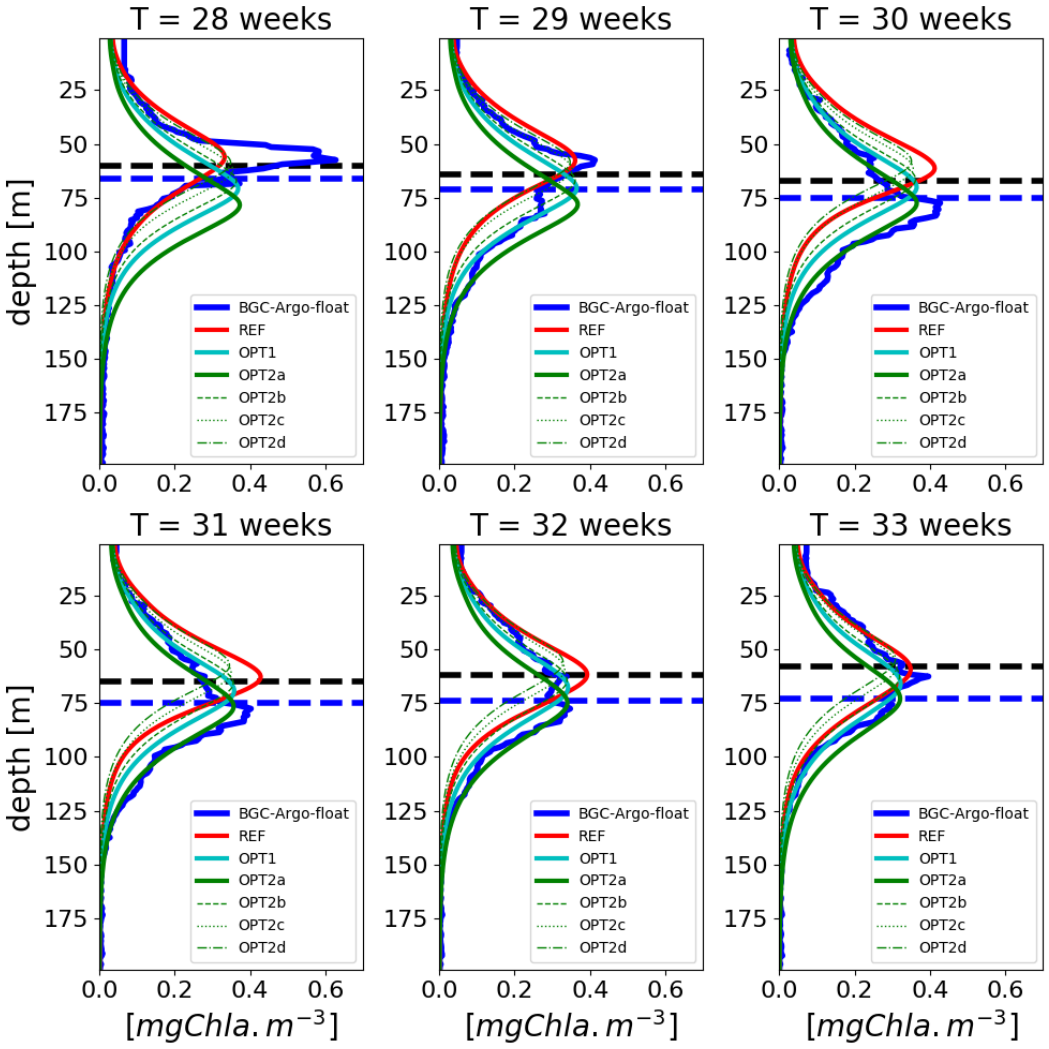

Figure 15. Example of a weekly time series of vertical profiles referred to lovbio035b BGC-Argo float (~~Fig.~~Figure 4) showing REF simulation and alternative bio-optical models OPT1 and OPT2 ~~, and~~ compared to BGC-Argo float ~~chlorophyll~~ Chl values (thicker line). The horizontal dashed blue line represents the euphotic depth z_{eu}, ~~defined as , where is~~ whereas the ~~surface irradiance. The horizontal~~ dashed black line indicates the depth where measured PAR ~~has a value of~~ equals 0.5 $\mathrm{molquanta\,m^{-2}\,day^{-1}}$ as identified in Mignot et al. (2014). The legend reports ~~the~~ model configurations listed in ~~Tab.~~Table 1.

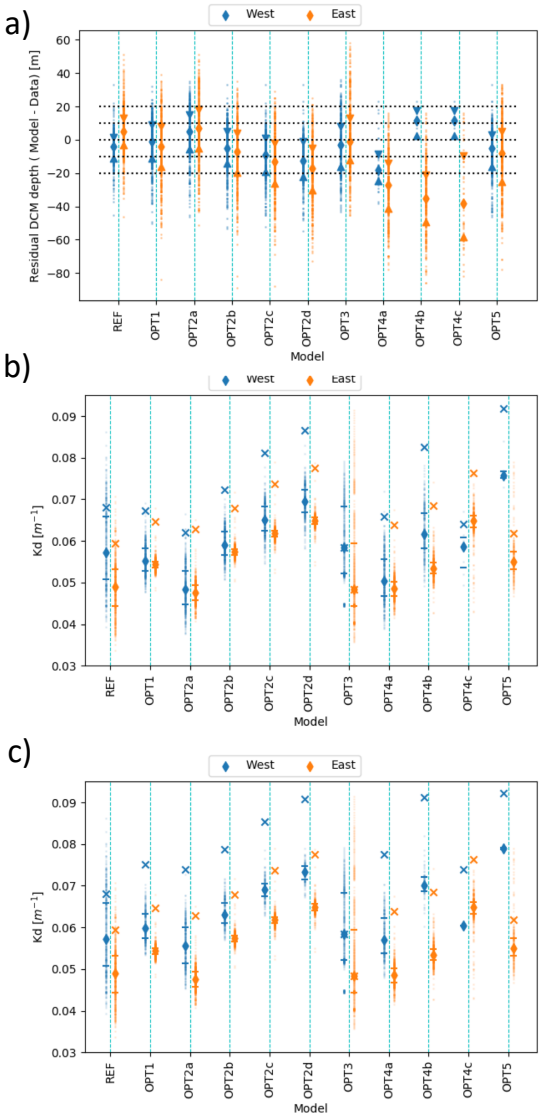

Figure 16. Panel a): Scatter plots of the residual difference between measured and modeled DCMs. The ~~x-axis~~ x-axis reports ~~the~~ model configurations listed in ~~Tab.~~Table 1. On the y-axis~~the median of the~~ , residuals' median values for ~~the~~ west (blue) and east (orange) profiles ~~is~~ are shown. Triangles indicate the 25th and 75th ~~percentile~~percentiles. Panel b): K_d for west and east subbasin during stratified period, diamonds indicate the median over the vertical column, 25th and 75th percentiles are the horizontal lines. Crosses show the maximum over the vertical column. Panel c) is the same as b) but with double initial nutrient concentrations for the western basin simulations.

~~Scatter plot comparing 0-25 m average surface chlorophyll versus BGC Argo float data for the stratified period condition, .~~

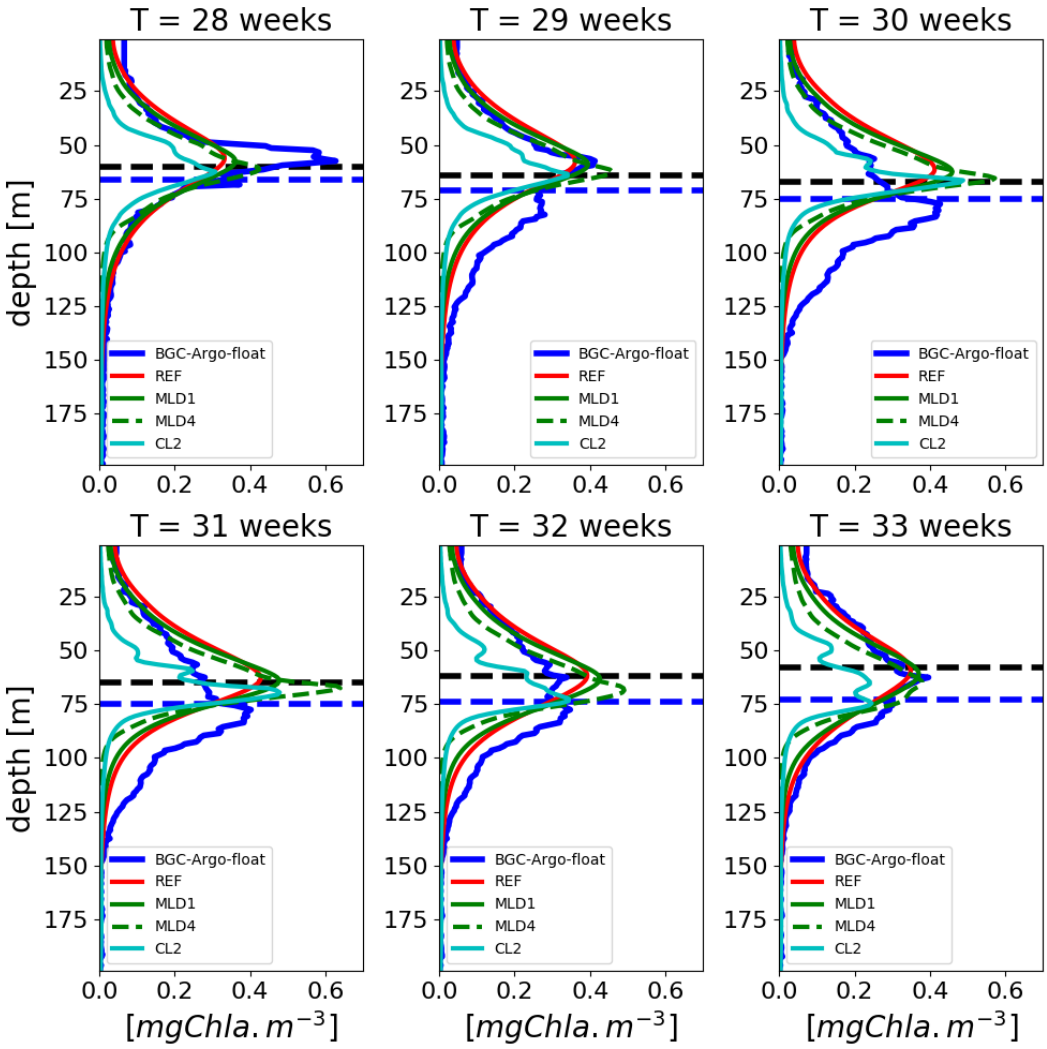

Figure 17. Example of a weekly time series of vertical profiles referred to lovbio035b BGC-Argo float (~~Fig.~~Figure 4) based on diel variability and constant daily light descriptions, ~~and~~ compared to BGC-Argo float ~~chlorophyll~~ Chl values (thicker blue line). The horizontal dashed blue line represents the euphotic depth z_{eu}, ~~defined as , where is~~ whereas the ~~surface irradiance. The horizontal~~ dashed black line indicates the depth where measured PAR ~~has a value of~~ equals 0.5 $\mathrm{molquanta\,m^{-2}\,day^{-1}}$ as identified in Mignot et al. (2014). The legend reports ~~the~~ model configurations listed in ~~Tab.~~Table 1.

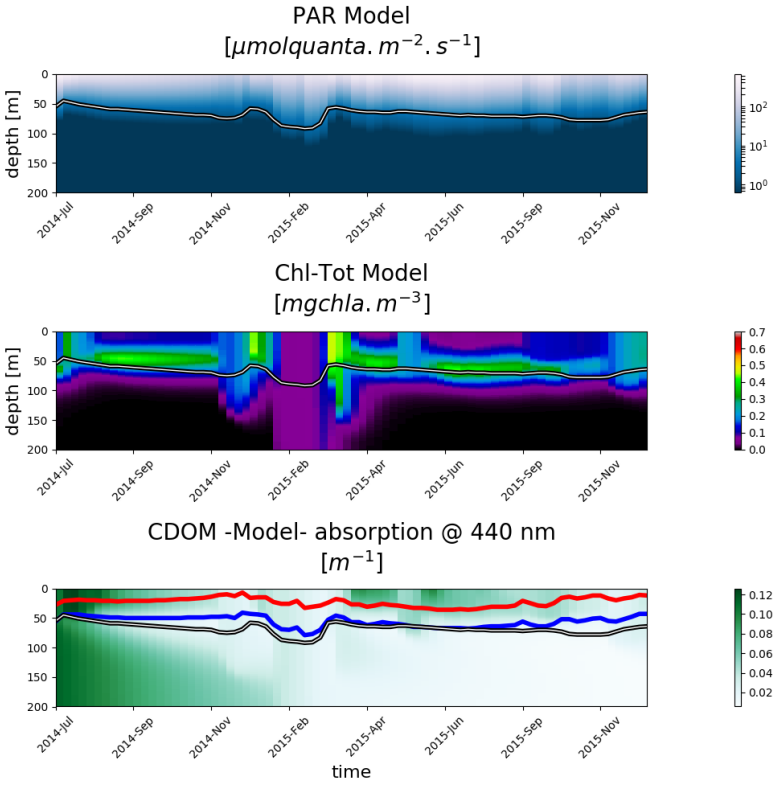

Figure 18. ~~Hovmoeller~~ Hovmöller diagrams for ~~BGC-Argo~~ BGC-Argo float lovbio068d (WMO code 6901648) showing: PAR (top), total chlorophyll (middle) and CDOM (bottom) simulated by model configuration OPT5. The white, red and blue lines depict the euphotic~~depth~~, ~~the~~ 100% ~~bleaching region~~ and ~~the~~ 10% bleaching ~~depth~~ depths respectively.